Two-nucleon one-loop corrections to pion double charge exchange within heavy baryon chiral perturbation theory

A. Misra[1,*] and D. S. Koltun[2,†]

[1]*Indian Institute of Technology, Kanpur 208 016, UP, India*
[2]*University of Rochester, Rochester, New York 14627*
(Received 6 November 1998; published 12 January 2000)

One-loop corrections at the two-nucleon level to pion double charge exchange scattering off a nuclear target at threshold are calculated within the framework of heavy baryon chiral perturbation theory. An estimate for the (two-nucleon) one-loop correction is obtained in the static limit and using an impulse approximation. We find a small (1.6%) increase relative to the leading order tree graphs.

I. INTRODUCTION

The effective field theory used most extensively to study QCD at low energies is generically referred to as chiral perturbation theory (ChPT). With the inclusion of baryons, the effective theory is called baryon ChPT (BChPT), whose nonrelativistic limit (with respect to the baryons) is referred to as heavy BChPT (HBChPT). So far, pion-nucleus scattering and production processes involving multiple nucleons with an arbitrary number of pions have been considered within HBChPT up to the tree level, with one-loop corrections only at the single-nucleon level (vertex corrections) [1,2]. In this paper, we perform a two-nucleon–one-loop calculation involving pion loops, with the pions being emitted and absorbed at different nucleons, which we believe has not been done before.

The goal of this paper is to determine the size of the one-loop contributions to pion double charge exchange (DCX) scattering at threshold on a nuclear target, relative to the tree graphs, in the framework of HBChPT. One of the motivations for this study is the fact that sizable one-loop (pion) contributions to π-π scattering and π-N scattering have been obtained in the framework of (HB)ChPT by previous authors [3,4]. Therefore it is natural to ask whether similar large contributions are found for a two-nucleon calculation involving pions in HBChPT to one loop. We shall find that this is not the case; the loop correction to the two-nucleon process is small, as expected for a chiral expansion.

The two-nucleon process considered is pion DCX:

$$\pi^+ + n + n \rightarrow \pi^- + p + p, \tag{1}$$

where the nucleons are in bound nuclear states. We consider only transitions to the DIAS (double isobaric analog states), e.g., ^{14}C$(\pi^+, \pi^-)^{14}$O (DIAS). The DIAS is that (normalized) state obtained by operating with $I_+ I_+$ on the target ground state, where I is the total isospin operator. The DCX contribution is much smaller than elastic scattering (^{14}C

$\rightarrow ^{14}$C) because while the former involves only the valence nucleons, the latter involves a coherent scattering of the core and the valence nucleons.

The reason for considering DCX at threshold is that it is dominated by two-nucleon processes, since single π-N scattering cannot contribute. It has been shown that the contribution of meson exchange currents (MEC) to DCX, although less than double scattering, is not all that small. (See [5] and references therein.) In the context of HBChPT, these results are at the leading order, or tree level. The second motivation of the present paper is to establish the size of the next-order correction to the two-nucleon MEC contribution to DCX.

In Sec. II, we introduce the theoretical background of single- and multinucleon HBChPT and discuss a chiral power counting rule due to Weinberg (including issues of reducibility of graphs, which is an additional complication arising at the multinucleon level). In Sec. III, we discuss the approximations involved in getting (analytical and numerical) estimates of the amplitudes for the tree and one-loop graphs for pion DCX. The relevant leading order tree graphs are evaluated in the framework of HBChPT and compared to an earlier calculation. In Sec. IV, we evaluate the two-nucleon one-loop corrections to the tree graphs of Sec. III. We then make a numerical estimate of the finite parts of the (two-nucleon) one-loop graphs, and make comparison with the tree graphs of Sec. III. In Sec. V, we discuss the renormalization of the one-loop graphs of Sec. IV using 2π–two-nucleon contact terms. Section VI summarizes and discusses the findings for the DCX problem. We include an estimate of the effect of vertex corrections on the tree graph amplitudes, based on earlier published work. There are two appendices: Appendix A presents the vertices written in terms of $\pi^\pm, \pi^0$ [rather than their Cartesian counterparts (as in [6]) as the former are more readily useful for calculation purposes] (Appendix A 1), and combinatoric factors Appendix A 2 for the one-loop π-NN graphs. Appendix B discusses the various one-loop integrals and related identities involving them, relevant to the DCX one-loop calculation, highlighting the ones that are new.

II. THEORETICAL BACKGROUND

In this section, we discuss the basic elements of HBChPT at the single- and multinucleon level that will be required later in the paper.

———————
*Electronic address: aalok@iitk.ac.in

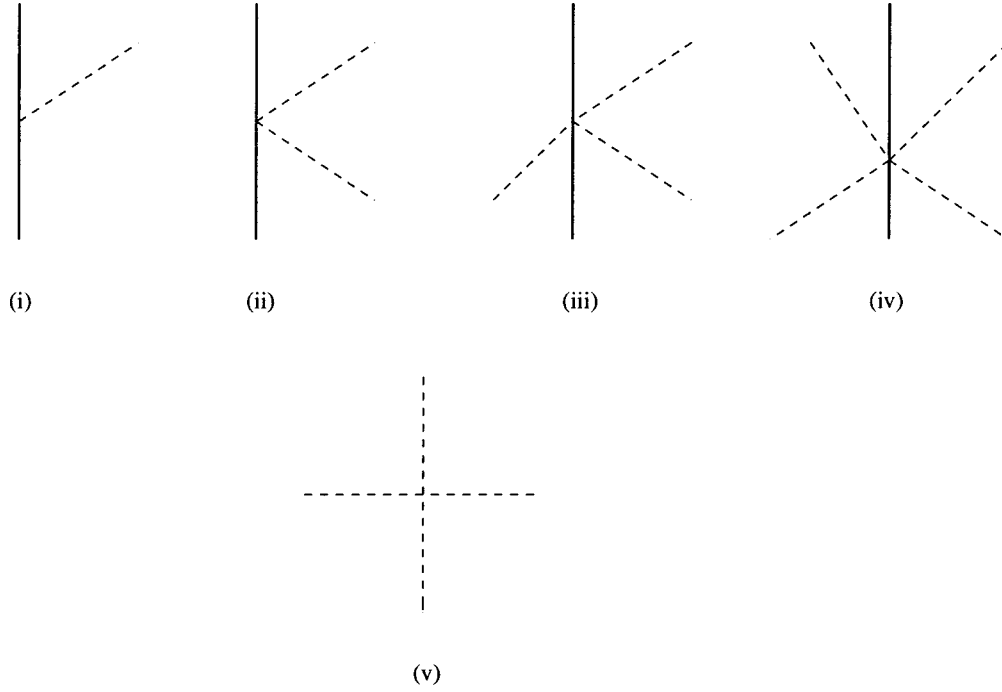†Electronic address: koltun@urhep.pas.rochester.edu

FIG. 1. Elementary vertices.

The leading order (LO) HBChPT Lagrangian that will be used in the calculations of the LO tree and one-loop graphs is given by

$$\bar{H}(i v \cdot D + g_A^0 S \cdot u)H + \frac{F^2}{4}(\langle \partial^\mu U^\dagger \partial_\mu U \rangle + M \langle U + U^\dagger - 2 \rangle),$$

(2)

where $g_A^0 \equiv$ axial-vector coupling constant, $F \equiv$ pion-decay constant and $M \equiv$ pion mass in the chiral limit. The trace in the nucleon isospin space is denoted by $\langle \ \rangle$ in Eq. (2).

The HBChPT Lagrangian is written in terms of the "upper component" H and its covariant adjoint $\bar{H}$, exponentially parametrized matrix-valued meson fields U, $u \equiv \sqrt{U}$, baryon ("v_μ, S_ν") and pion-field-dependent ("$D_\mu, u_\nu, \chi_\pm$") building blocks defined below:

$$H \equiv e^{im v \cdot x} \frac{1}{2}(1 + \slashed{v}) \psi,$$

(3)

where ψ is the Dirac spinor and m is the nucleon mass,

$$v_\mu \equiv \text{nucleon four-velocity parameter},$$

$$S_\nu \equiv \frac{i}{2} \gamma^5 \sigma_{\nu\rho} v^\rho \equiv \text{Pauli-Lubanski spin operator};$$

(4)

$$U = \exp\left(i \frac{\phi}{F_\pi}\right), \quad \text{where} \quad \phi \equiv \vec{\pi} \cdot \vec{\tau},$$

(5)

where $\vec{\tau}$ are the nucleon isospin generators; $D_\mu = \partial_\mu + \Gamma_\mu$ where $\Gamma_\mu \equiv \frac{1}{2}[u^\dagger, \partial_\mu u]$; $u_\mu \equiv i(u^\dagger \partial_\mu u - u \partial_\mu u^\dagger)$.

The $m\pi$-$\bar{N}N$ vertices, $m = 1, 3$, are constructed from the Yukawa term:

$$g_A^0 \bar{H} S \cdot u^{(1,3)} H$$

(6)

(where the superscript on u_μ represents the powers of the pion field). The 2π-$\bar{N}N$ vertex is constructed from the Dirac term:

$$i \bar{H} v \cdot D^{(2)} H \equiv i \bar{H} v \cdot \Gamma^{(2)} H$$

(7)

(where the superscripts on D_μ and Γ_μ represent the powers of the pion field).

The four-pion vertex is constructed from the nonlinear sigma model Lagrangian $\equiv$ LO ChPT Lagrangian:

$$\frac{F^2}{4}(\langle \partial^\mu U^\dagger \partial_\mu U \rangle + M^2 \langle U + U^\dagger - 2 \rangle).$$

(8)

For more details, refer to Appendix A.

The elementary vertices from which the tree and the one-loop graphs of Secs. II and III have been constructed, are drawn in Fig. 1. However, the calculations in the chiral perturbation expansion are renormalized to the chiral order of the expansion. The Weinberg chiral power counting relation (WCPCR, [7,8]) is used for a systematic classification of the relevant tree and one-loop graphs. The relation determines the overall chiral order of irreducible graphs in terms of the total number of incoming or outgoing nucleons (the two are the same because of baryon number conservation), the total number of loops, the chiral order of the vertices, and connectedness of the graphs, as discussed below. Here is the WCPCR:

$$\nu = 4 - N + 2(L - C) + \sum_i v_i \left(\frac{n_i}{2} + d_i - 2\right),$$

(9)

where $\nu\equiv$ overall chiral order of a graph, $N\equiv$ total number of incoming/outgoing nucleons, $L\equiv$ number of loops, $C\equiv$ number of separately connected pieces of the graph, $v_i\equiv$ the number of vertices of type i, $n_i\equiv$ the number of incoming *and* outgoing nucleons at the ith vertex and $d_i\equiv$ is the number of derivatives or powers of M_π. From baryon number conservation, $n_i\equiv 2$ or 0.

Graphs which violate relation (9) because of anomalously small denominators are referred to as reducible by Weinberg [8]. This class includes graphs whose energy denominators in old-fashioned time-ordered perturbation theory are of the order of M_π^2/m rather than M_π. These graphs arise in the context of NN or many-nucleon scattering, without external pions. (For a recent treatment of the NN scattering problem which deals with problems of the Weinberg scheme, see [9,10].) However, for pion scattering on NN pairs, as in the present paper, all graphs are irreducible, as can be seen from the discussion of [8]. In Secs. III and IV, WCPCR will be used to determine the overall chiral order of the tree and one-loop graphs.

The lowest order tree graphs for DCX, based on the LO vertices (6)–(8), will be shown to be of chiral order $\nu=0$ (see Sec. III B). The one-loop corrections at the $2N$ level, which are the main subject of this paper, are of order $\nu=2$ (see Sec. IV). To this same order, there are also corrections to the LO vertices, which have already been obtained in (HB)ChPT (see [3,4,11]) as renormalized effective interactions, with a number of low-energy constants (LECs). These LECs are to be fixed from experiment, but are not in fact all known. (For the π-π vertex, the LECs of $\nu=2$ are ''almost'' all determined [3]. For $\pi-N$, the information is less complete, but has been supplemented by theoretical arguments [4,6,11] for on-shell nucleons.)

However, we do know the renormalized values of the pion and nucleon masses, the axial-vector coupling constant, and the pion-decay constant. For the purpose of numerical calculation of the analytical expressions for the tree and one-loop graphs later in the paper, we use

$$M_\pi = 139.57 \text{ MeV}, \quad F_\pi = 93 \text{ MeV}, \quad g_A = 1.26. \tag{10}$$

Renormalizing these constants, including the nucleon mass m, to one-loop (in the π-N and π-π interactions) gives the following relations to the corresponding quantities in the chiral limit g_A^0, m^0, M, F:

$$g_A = g_A^0[1+\rho_g M^2],$$

$$m = m^0[1+\rho_m M^2],$$

$$M_\pi^2 = M^2[1+\rho_M M^2], \tag{11}$$

$$F_\pi = F[1+\rho_F M^2],$$

where the ρ_i include some of the (HB)ChPT LECs.

It is also known that the one-loop corrections to the π-π vertex give contributions of about 25% of order $\nu=2$. Similar corrections to the $m\pi$-N vertices (with $m=1,2,3$) are as

large as 10–30 % [3,4,11]. So we know the order of magnitude of the $\nu=2$ corrections to the LO DCX (tree) amplitudes from the one-loop vertex contributions, but cannot determine these corrections completely, without the undetermined LECs.

For that reason, we shall use the vertices (6)–(8), with the renormalized values (10) for the tree calculation in Sec. III, omitting unknown (but significant) corrections of the same order. The one-loop corrections at the $2N$ level are calculated in Sec. IV with the same vertices.

III. DCX SCATTERING AMPLITUDES; TREE GRAPHS

In this section we discuss the approximations that will be made in evaluation of tree and one-loop graphs for DCX scattering of pions off a nuclear target, set up the notations and calculate the amplitudes for the leading order (DCX) tree graphs.

A. Notations and approximations

The scattering matrix element S_{fi} is defined as

$$S_{fi} = -i(2\pi)^4\delta^{(4)}(P_f-P_i)\frac{1}{(2\pi)^9 M_\pi}\mathcal{M}. \tag{12}$$

In Eq. (12), the nuclear scattering amplitude $\mathcal{M}$ is defined as the matrix element of a two-body operator T:

$$\mathcal{M}\equiv\langle\psi_o, I=1, \ I_3=1|T\tau_+^{(1)}\tau_+^{(2)}|\psi_i, I=1, \ I_3=-1\rangle$$

$$=\langle\psi_o|T|\psi_i\rangle\times\langle I=1, \ I_3=1|\tau_+^{(1)}\tau_+^{(2)}|I=1, \ I_3=-1\rangle, \tag{13}$$

where we assume a target with $2n+$ isoscalar core ($I=1, \ I_3=-1$); then the DIAS has $2p+$ isoscalar core ($I=1, \ I_3=1$). The isospin matrix element in the second line of Eq. (13) equals unity, and will be omitted in the following.

If $p_{1,2}^\mu$ were the four-momenta of the incoming nucleons, $p_{3,4}^\mu$ the four-momenta of the outgoing nucleons, and $q_{1,2}^\mu$ the four-momenta of the incoming and outgoing pions (respectively) then

$$\mathcal{M} = \int\prod_{i=1}^{4} d^3p_i\langle\psi_o(p_3,p_4)|T|\psi_i(p_1,p_2)\rangle. \tag{14}$$

The nucleons are in a relative $l=0$ state ($l=0$ state being the dominant partial wave for ground states) and hence from Pauli's exclusion principle, the spin of the incoming and outgoing nuclear states must be equal to zero. Hence, from here on, for both tree and one-loop graphs, we will simplify the structure of the transition operator T assuming that eventually one is going to take it's expectation value with respect to $|l=S=0\rangle$ nuclear states.

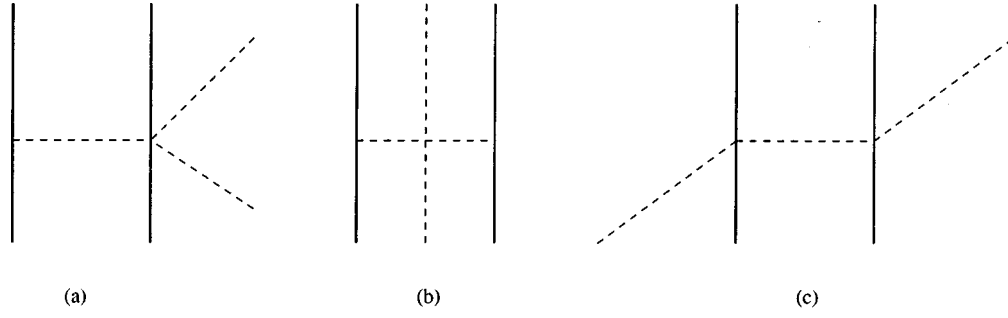The following will be used extensively in the same context:

FIG. 2. Tree graphs.

$$\langle S=0|(\vec{\sigma}^{(1)}\cdot\vec{q})(\vec{\sigma}^{(2)}\cdot\vec{q})|S=0\rangle=\langle\vec{\sigma}^{(1)}\cdot\vec{\sigma}^{(2)}\rangle_{S=0}\frac{\vec{q}^2}{3}=-\vec{q}^2.$$
(15)

Following [1] and [2], first the velocity parameters of the two participating nucleons are both chosen to have the static limit values, with only a nonvanishing time component, i.e., $v_1^\mu=v_2^\mu=(1,\vec{0})$. Second, the nucleons will be treated as if they were on shell (sometimes referred to as impulse approximation). In the HBChPT formalism, p^0 denotes only the contribution to the time component of the total nucleon momenta ($\equiv mv+p$), *in addition* to the rest mass energy m (for the choice of the nucleon velocity to possess only a nonzero time component). In the present case $p^0=E_B$, which as stated above, we drop. Then if we go to the c.m. frame of the nucleons,

$$p_1^\mu=(0,\vec{p}); \quad p_2^\mu=(0,-\vec{p}); \quad p_3^\mu=(0,\vec{p}');$$

$$p_4^\mu=(0,-\vec{p}'); \quad q_1^\mu=q_2^\mu=(M_\pi,\vec{0}).$$
(16)

(Note: The external pions are at zero kinetic energy [threshold].)

For this paper, we shall only evaluate $\langle S=0|T|S=0\rangle$. $\mathcal{M}$ will be estimated by calculating $\langle S=0|T|S=0\rangle$ at a typical point:

$$\vec{P}^2=M_\pi^2,$$
(17)

where $\vec{P}\equiv\vec{p}'-\vec{p}$. This is a reasonable kinematic point because the internucleon separation in a nucleus averaged over the nuclear wave function is roughly M_π^{-1}. Then

$$\mathcal{M}\approx\langle S=0|T(\vec{P}^2=M_\pi^2)|S=0\rangle$$

$$\times\int\prod_{i=1}^4 d^3p_i\langle\psi_o(p_3;p_4)|\psi_i(p_1;p_2)\rangle$$

$$=\langle S=0|T(\vec{P}^2=M_\pi^2)|S=0\rangle,$$
(18)

where the last line follows because the overlap integral is unity for $\psi_o\equiv$ DIAS of ψ_i.

B. Tree graphs

The connected tree graphs are of overall $O(q^0)$, as follows from the chiral counting law (9), because for them $N=2$, $L=0$, $C=1$, $n_i=2$ or 0, $d_i=1$ or 2. The tree graphs have been constructed from the first three and the fifth elementary vertices of Fig. 1. They are drawn in Fig. 2. For LO graphs, all the vertices have to be of LO, i.e., $O(q)m\pi$ $-\bar{N}N(m=1,2,3)$ and $O(q^2)$ 4 π vertices. Using the exponential parametrization for the matrix-valued meson field, $\mathcal{L}_{HBChPT}$ and $\mathcal{L}_{ChPT}$ are written down explicitly in terms of the pion triplet fields: $\pi^0,\pi^\pm$, and p, n fields [refer to Appendix A 1].

The S matrix for Eq. (1) can be calculated in perturbation theory using standard Feynman-diagram techniques. For the nth order term, $S^{(n)}$, a combinatoric factor f is defined via

$$S^{(n)}=\frac{i^n}{n!}\int\prod_{k=1}^n d^4x_k\mathcal{T}\left(\prod_{i=1}^n\sum_j\mathcal{L}_j^I(x_i)\right)$$

$$=fi^n\int\prod_{k=1}^n d^4x_k\mathcal{T}\left(\prod_{i=1}^n\mathcal{L}_i^I(x_i)\right)$$
(19)

($\mathcal{T}\equiv$ time-ordering operator), where one uses $\mathcal{T}(AB)=\mathcal{T}(BA)$, where $A,B\equiv$ bosonic fields or fermionic bilinears.

One can show that the combinatoric factors for tree graphs of Fig. 2 are

contact graph, Fig. 2(a): $\quad f=1,$

Pole graph, Fig. 2(b): $\quad f=\frac{1}{2},$
(20)

double-scattering graph Fig. 2(c): $\quad f=\frac{1}{2}.$

The amplitudes for the tree graphs are written in terms of Pauli spinors (to which H and $\bar{H}$ reduce in the static limit) and the pionic field $\phi^-\tau_+$ [see Eq. (54)].

Using also Eqs. (16), (17), and (20), the amplitudes for the tree graphs are expressed as operators written in terms of **1** and $\vec{\sigma}^{(1)}\cdot\vec{P}\vec{\sigma}^{(2)}\cdot\vec{P}$.

What follows are expressions for T and $\langle S=0|T(\vec{P}^2=M_\pi^2)|S=0\rangle$.
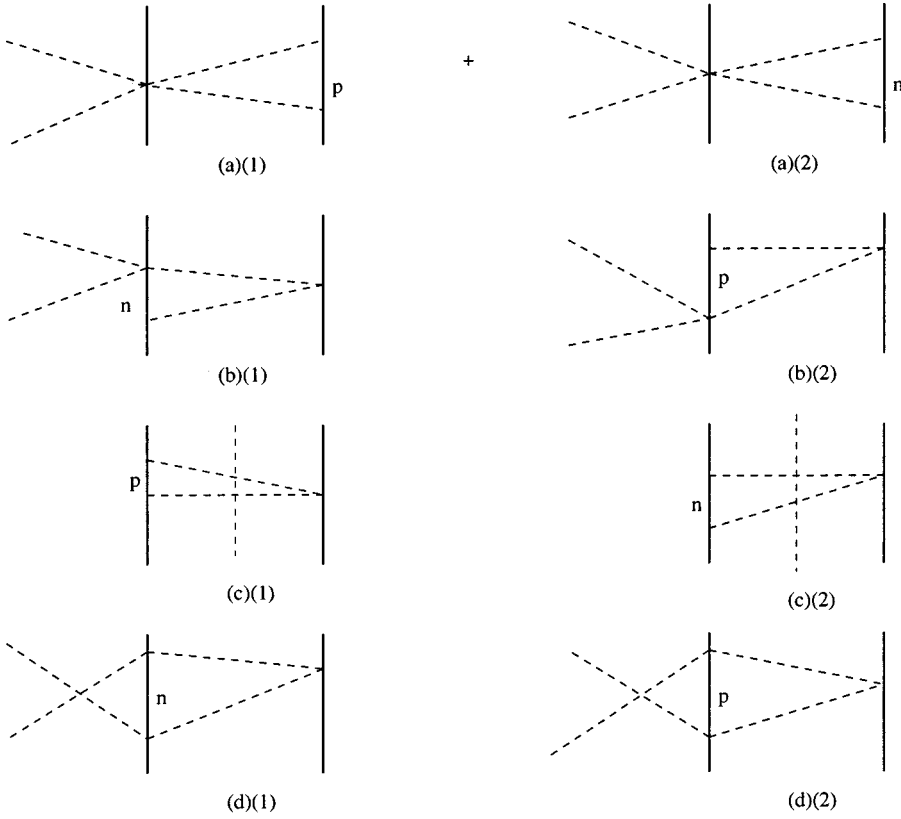
(a) Contact graph, Fig. 2(a):

FIG. 3. Two-nucleon–one-loop graphs (a)–(d).

$$T_{[a]} = 2(\sqrt{2})^4 \frac{g_A^2}{24F_\pi^4} \frac{\vec{\sigma}^{(1)} \cdot \vec{P} \vec{\sigma}^{(2)} \cdot \vec{P}}{M_\pi^2 + \vec{P}^2}, \quad (21)$$

which using Eqs. (15) and (17), gives

$$\langle S=0 | T_{[a]}(\vec{P}^2 = M_\pi^2) | S=0 \rangle$$

$$= -\frac{g_A^2}{6F_\pi^4} = -1.42 \times 10^{-8} \text{MeV}^{-4}. \quad (22)$$

(b) Pole graph, Fig. 2(b):

$$T_{[b]} = (\sqrt{2})^6 \frac{g_A^2}{24F_\pi^4} [2M_\pi^2 - \vec{P}^2] \frac{\vec{\sigma}^{(1)} \cdot \vec{P} \vec{\sigma}^{(2)} \cdot \vec{P}}{[M_\pi^2 + \vec{P}^2]^2}, \quad (23)$$

which using Eqs. (15) and (17), gives

$$\langle S | T_{[b]}(\vec{P}^2 = M_\pi^2) | S=0 \rangle = -\frac{g_A^2}{12F_\pi^4} = -6.3 \times 10^{-9} \text{ MeV}^{-4}. \quad (24)$$

(c) Double-scattering graph, Fig. 2(c):

$$T_{[c]} = -(\sqrt{2})^4 \frac{M_\pi^2}{8F_\pi^4} \frac{1}{\vec{P}^2}, \quad (25)$$

which using Eq. (17), gives

$$\langle S=0 | T_{[c]}(\vec{P}^2 = M_\pi^2) | S=0 \rangle$$

$$= -\frac{1}{2F_\pi^4} = -2.67 \times 10^{-8} \text{ MeV}^{-4}. \quad (26)$$

Thus, the total tree-graph amplitude is

$$\langle S=0 | T_{\text{total}}[\text{tree}](\vec{P}^2 = M_\pi^2) | S=0 \rangle$$

$$= -\frac{1}{4F_\pi^4} (g_A^2 + 2) = -4.81 \times 10^{-8} \text{ MeV}^{-4}. \quad (27)$$

An older form of chiral Lagrangian that predates QCD was given by Olsson and Turner (OT) [12], and has been used for tree calculations, e.g., of DCX [5]. It consists of the minimum number of derivatives of the pion and nucleon fields, with two undetermined (model dependent) parameters. It can be easily shown that the OT effective Lagrangian is equivalent to the LO vertices obtained from Eqs. (6) and (8), with the OT parameters taken to be ''ξ, η''$=(\frac{2}{3}, -\frac{1}{6})$. Therefore, the tree-graph calculations of this section should agree (as they indeed do) with the expressions obtained in [5] for the transition operators for ''forward scattering'' for the ''pion-contact'' and ''pion-pole'' graphs, using the same values of the OT parameters. This provides a check on the tree-level calculation using HBChPT.
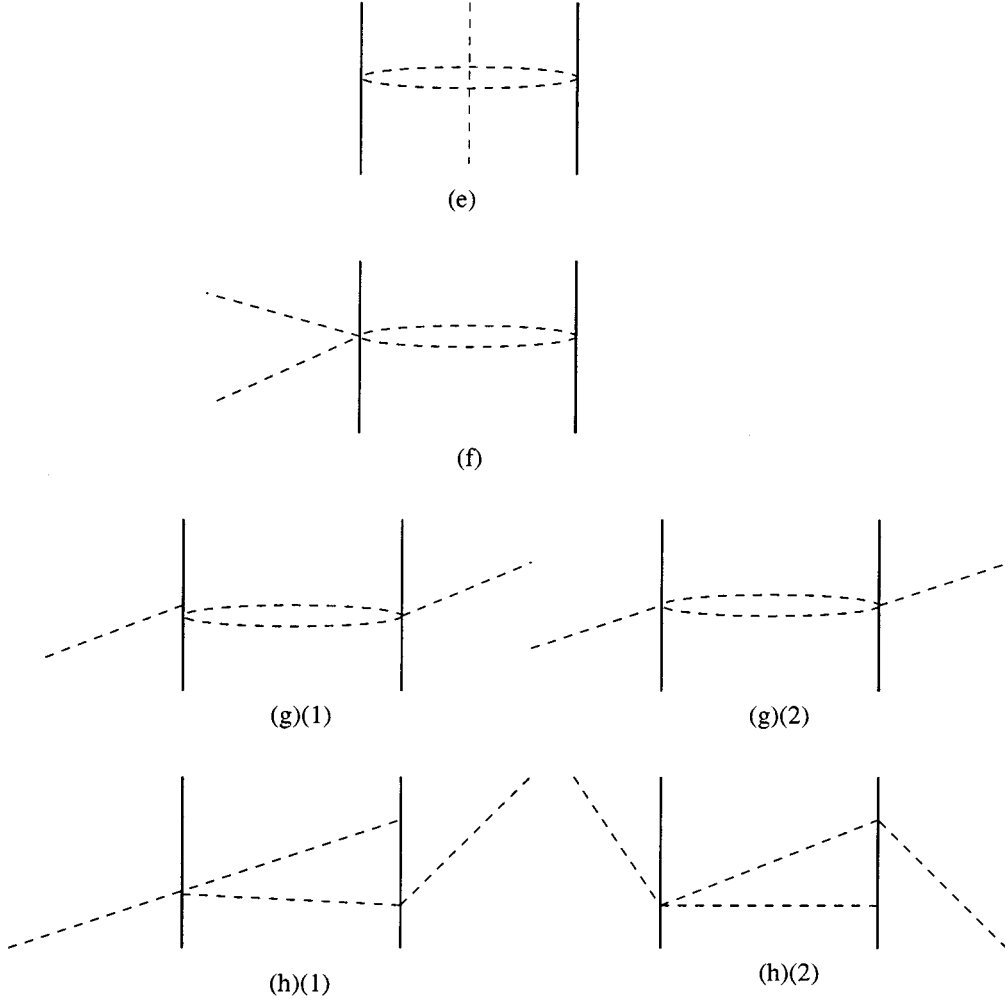
FIG. 4. Two-nucleon–one-loop graphs (e)–(h).

IV. ONE-LOOP GRAPHS FOR π-NN

In this section, we discuss how to evaluate one-loop corrections to the tree graphs (that were evaluated in Sec. III) for pion DCX, in the framework of HBChPT. Loop graphs, in the present context, involve the emission of two or more pions from one nucleon leg and their absorption at another nucleon leg (for multinucleon processes). For evaluation of the one-loop integrals that occur in the two-nucleon–one-loop graphs, use has been made of dimensional regularization in which the space-time dimension ''d'' is allowed to vary continuously, and expressions obtained after integration are expanded around $d=4$.

One gets eight one-loop graphs using all five of the elementary $m\pi$-$\bar{N}N(m=1,2,3,4)$ and 4-π vertices of Fig. 1. They are drawn in Figs. 3 and 4. The uncrossed counterpart of Fig. 3(d) is not included because it belongs to the class of multiple-scattering graphs involving at least three nucleons, which are not considered in this paper. For Fig. 4(h), if the two pions exchanged were π^0's, then the amplitudes would vanish in the static limit.

The leading order connected two-nucleon one-loop graphs (for DCX) are of $O(q^2)$, as can be seen from Eq. (9), because for these graphs, $N=2$, $L=C=1$, (n_i, d_i)

$=(2, 1)$ or $(0, 2)$. The vertices corresponding to the interaction of an even number of pions (two or four for our purpose) with nucleons, are obtained from the Dirac term (7), while the vertices corresponding to the interaction of an odd number of pions (one or three for our purpose) with nucleons, are obtained from the Yukawa term (6). The LO($\equiv O(q^2)$) ChPT Lagrangian (8), which is equivalent to the nonlinear σ model, is used for the 4π vertex. However, we do use the renormalized constants (10), which introduces some corrections of higher order. For details refer to Appendix A 1.

The one-loop amplitudes are written using standard Feynman rules. The expressions for the T-matrix elements for the eight one-loop graphs for fixed momenta of the external nucleons legs are given below. For notational convenience, $H_{neutron}(p_{1,2})$ is represented as $n(p_{1,2})$, and $\bar{H}_{proton}(p_{3,4})$ is represented as $\bar{p}(p_{3,4})$. Including the combinatoric factors ''f'' of Eq. (19), one arrives at the expressions below for $T_{[j]}$, $j=a,\ldots,h$. They are first written in a covariant notation except that the two velocities of the two nucleons are chosen to be the same, i.e., $v_1=v_2\equiv v$ (as in Sec. III). Then the static limit kinematics (16) is applied. (The combinatoric factors are given first for each diagram, and are obtained in Appendix A 2.)

(a)

$$T_{[a]} = \frac{(\sqrt{2})^6 g_A^2}{96 F_\pi^6} \frac{1}{i} \int \frac{d^d k}{(2\pi)^d} \left[\frac{\bar{p}(p_3) \boldsymbol{v} \cdot (2p_2 - 2p_4) n(p_1) \bar{p}(p_4) S^{(2)} \cdot (p_4 - p_2 + k) S^{(2)} \cdot k n(p_2)}{(\boldsymbol{v} \cdot (k - p_2) - i\epsilon)(M_\pi^2 - k^2 - i\epsilon)(M_\pi^2 - (p_4 - p_2 + k)^2 - i\epsilon)} \right]. \tag{28}$$

Using Eq. (16), Eq. (28) vanishes because $\boldsymbol{v} \cdot (p_2 - p_4) \to 0$.

(b)

$$T_{[b]} = 2 \frac{(\sqrt{2})^6 g_A^2}{96 F_\pi^6} \frac{1}{i} \int \frac{d^d k}{(2\pi)^d} \left[\frac{\bar{p}(p_3) S^{(1)} \cdot k S^{(1)} \cdot (q_1 - q_2 + 2p_4 - 2p_2 + 2k) n(p_1) \bar{p}(p_4) \boldsymbol{v} \cdot (p_4 - p_2 + 2k) n(p_2)}{(\boldsymbol{v} \cdot (k - p_3) - i\epsilon)(M_\pi^2 - k^2 - i\epsilon)[M_\pi^2 - (k + p_4 - p_2)^2 - i\epsilon]} \right.$$

$$\left. + \frac{\bar{p}(p_3) S^{(1)} \cdot (q_1 - q_2 + 2p_4 - 2p_2 - 2k) S^{(1)} \cdot k n(p_1) \bar{p}(p_4) \boldsymbol{v} \cdot (p_4 - p_2 - 2k) n(p_2)}{(\boldsymbol{v} \cdot (k - p_1) - i\epsilon)(M_\pi^2 - k^2 - i\epsilon)[M_\pi^2 - (k + p_2 - p_4)^2 - i\epsilon]} \right]. \tag{29}$$

(c)

$$T_{[c]} = \frac{(\sqrt{2})^8 g_A^2 M_\pi^2}{96 F_\pi^6} \frac{1}{i} \int \frac{d^d k}{(2\pi)^d} \left[\frac{\bar{p}(p_3) S^{(1)} \cdot (p_3 - p_1 + k) S^{(1)} \cdot k n(p_1)}{(\boldsymbol{v} \cdot (k - p_1) - i\epsilon)} + \frac{\bar{p}(p_3) S^{(1)} \cdot k S^{(1)} \cdot (p_3 - p_1 + k) n(p_1)}{(\boldsymbol{v} \cdot (k + p_3) - i\epsilon)} \right]$$

$$\times \left[\frac{[4 q_1 \cdot q_2 + 2k \cdot (q_1 - q_2 + k)] \bar{p}(p_4) \boldsymbol{v} \cdot (q_1 - q_2 + p_3 - p_1 + 2k) n(p_2)}{[M_\pi^2 - (k + q_1 - q_2) - i\epsilon](M_\pi^2 - k^2 - i\epsilon)[M_\pi^2 - (k - [p_1 - p_3])^2 - i\epsilon]} \right]. \tag{30}$$

(d) One can show that the contributions of $(d)(1)$ and $(d)(2)$ [in Fig. 3(d)] are equal, giving an overall factor of 2:

$$T_{[d]} = -\frac{2}{3} \frac{g_A^2 (\sqrt{2})^6}{256 F_\pi^6} \frac{1}{i} \int \frac{d^d k}{(2\pi)^d} \left[\frac{\bar{p}(p_3) \boldsymbol{v} \cdot (q_1 - p_2 + p_4 - k) \boldsymbol{v} \cdot (k - q_2) n(p_1) \bar{p}(p_4) \boldsymbol{v} \cdot (p_2 - p_4 + 2k) n(p_2)}{(\boldsymbol{v} \cdot (k + q_2 - p_1) - i\epsilon)(M_\pi^2 - k^2 - i\epsilon)[M_\pi^2 - (k - [p_4 - p_2])^2 - i\epsilon]} \right]. \tag{31}$$

(e)

$$T_{[e]} = \frac{(\sqrt{2})^8}{384 F_\pi^6} \frac{1}{i} \int \frac{d^d k}{(2\pi)^d} \left[\frac{[4 q_1 \cdot q_2 + 2k \cdot (q_1 - q_2 + k)]}{(M_\pi^2 - k^2 - i\epsilon)[M_\pi^2 - (q_1 - q_2 + k)^2 - i\epsilon][M_\pi^2 - (k - [p_1 - p_3])^2 - i\epsilon]} \right]$$

$$\times [\bar{p}(p_3) \boldsymbol{v} \cdot (p_1 - p_3 - 2k) n(p_1) \bar{p}(p_4) \boldsymbol{v} \cdot (q_1 - q_2 + p_3 - p_1 + 2k) n(p_2)]. \tag{32}$$

(f)

$$T_{[f]} = 2 \frac{(\sqrt{2})^6}{384 F_\pi^6} \frac{1}{i} \int \frac{d^d k}{(2\pi)^d} \left[\frac{\bar{p} \boldsymbol{v} \cdot (q_2 - q_1 + 2p_2 - 2p_4 + 2k) n(p_1) \bar{p}(p_4) \boldsymbol{v} \cdot (p_2 - p_4 + 2k) n(p_2)}{(M_\pi^2 - k^2 - i\epsilon)[M_\pi^2 - (k - [p_4 - p_2])^2 - i\epsilon]} \right]. \tag{33}$$

(g)

$$T_{[g]} = -g_A^2 \frac{(\sqrt{2})^6}{144 F^6} \frac{1}{i} \int \frac{d^d k}{(2\pi^d)} \left(\frac{\bar{p}(p_3) S^{(1)} \cdot (p_1 - p_3 + q_1) n(p_1) \bar{p}(p_4) S^{(2)} \cdot (p_1 - p_3 + q_1) n(p_2)}{(M_\pi^2 - k^2 - i\epsilon)[M_\pi^2 - (k - [q_1 + p_1 - p_3])^2 - i\epsilon]} \right.$$

$$\left. + \frac{\bar{p}(p_3) S^{(1)} \cdot (p_3 - p_1 + 3k) n(p_1) \bar{p}(p_4) S^{(2)} \cdot (2p_2 - 2p_4 - 3q_2 + 3k) n(p_2)}{(M_\pi^2 - k^2 - i\epsilon)[M_\pi^2 - (k - [q_1 + p_1 - p_3])^2 - i\epsilon]} \right). \tag{34}$$

(h)

$$T_{[h]} = 2 \frac{g_A^2 (\sqrt{2})^6}{96 F_\pi^6} \frac{1}{i} \int \frac{d^d k}{(2\pi)^d} \left(\frac{\bar{p}(p_3) S^{(1)} \cdot (p_2 - p_4 + q_1 - q_2 + 3k) n(p_1) \bar{p}(p_4) S^{(2)} \cdot k \boldsymbol{v} \cdot (k + p_2 - p_4 - 2q_2) n(p_2)}{(\boldsymbol{v} \cdot (k - p_4) - i\epsilon)[M_\pi^2 - (k - [p_4 - p_2 + q_2])^2 - i\epsilon](M_\pi^2 - k^2 - i\epsilon)} \right.$$

$$\left. - \frac{\bar{p}(p_3) S^{(1)} \cdot (p_2 - p_4 + q_1 - q_2 - 3k) n(p_1) \bar{p}(p_4) \boldsymbol{v} \cdot (p_4 - p_2 - 2q_1 + k) S \cdot k n(p_2)}{(\boldsymbol{v} \cdot (k - p_2) - i\epsilon)(M_\pi^2 - k^2 - i\epsilon)[M_\pi^2 - (k - [q_1 + p_2 + p_4])^2 - i\epsilon]} \right) + q_1 \leftrightarrow -q_2. \tag{35}$$

TABLE I. List of one-loop integrals in Eqs. (37)–(47).

I_k	Integrals of Appendix B	Equation	Numerical value of UV-finite part at $\mu=1$ GeV
I_1	$\mathcal{J}^{\pi\pi}(-M_\pi^2,M_\pi^2)$	(B9)	0.018
I_2	$\mathcal{J}_1^{\pi\pi}(-M_\pi^2,M_\pi^2)$	(B19)	0.009
I_3	$\mathcal{J}_2^{\pi\pi}(-M_\pi^2,M_\pi^2)$	(B23)	$0.014M_\pi^2$
I_4	$\mathcal{J}_3^{\pi\pi}(-M_\pi^2,M_\pi^2)$	(B25)	0.006
I_5	$\dfrac{\partial}{\partial M^2}\mathcal{J}_1^{\pi\pi}(-M_\pi^2,M^2)_{M^2=M_\pi^2}$	(B21)	$-0.004M_\pi^{-2}$
I_6	$\dfrac{\partial}{\partial M^2}\mathcal{J}_2^{\pi\pi}(-M_\pi^2,M^2)\big|_{M^2=M_\pi^2}$	(B27)	0.002
I_7	$\dfrac{\partial}{\partial M^2}\mathcal{J}_3^{\pi\pi}(-M_\pi^2,M^2)\big|_{M^2=M_\pi^2}$	(B29)	-0.004
I_8	$\mathcal{J}^{\pi\pi}(0,M_\pi^2)$	(B10)	0.019
I_9	$\mathcal{J}_2^{\pi\pi}(0,M_\pi^2)$	(B8),(B17)	0.013
I_{10}	$\mathcal{J}_3^{\pi\pi}(0,M_\pi^2)$	(B10),(B18)	0.006
I_{11}	$\gamma_0(-M_\pi,0,-M_\pi^2)$	(B13)	$0.019M_\pi^{-1}$
I_{12}	$\gamma_2(0,-M_\pi,0)-\gamma_2(0,M_\pi,0)$	(B31)	$0.025M_\pi^{-1}$
I_{13}	$\gamma_3(0,-M_\pi,0)-\gamma_3(0,M_\pi,0)$	(B34)	$-0.022M_\pi$
I_{14}	$\gamma_5(0,-M_\pi,0)-\gamma_5(0,M_\pi,0)$	(B37)	$0.022M_\pi^{-1}$

The amplitudes for the eight one-loop graphs are now written in terms of 11 of the 13 one-loop integrals discussed in Eqs. (B1)–(B3) of Appendix B. They, like the tree graphs of Sec. III, are evaluated in Eq. (17). The Pauli matrices $\vec{\sigma}^{(1),(2)}$ come from the nonrelativistic reduction of $S_\mu^{(1),(2)}$. The expressions below are written in terms of Pauli spin operators, and will be evaluated for $\langle S=0|T|S=0\rangle$. For graphs (a)–(f), the spin operator is unity; for (g) and (h), we use Eq. (15).

Using dimensional regularization, the ''L'' in the expressions below is the UV-divergent portion of the loop integrals and is defined by

$$L\equiv\frac{\mu^{d-4}}{16\pi^2}\left(\frac{1}{d-4}-\frac{1}{2}[1+\Gamma'(1)+\ln(4\pi)]\right),\quad(36)$$

where d is the dimension parameter and μ is the renormalization point, which is taken to be of the order of the nucleon mass. Following [11] we use $\mu=1$ GeV, and also vary the value by ±0.5 GeV to test the sensitivity of the results to this choice.

The momentum loop integrals are then rewritten in terms of the one-loop integrals of Eqs. (B1)–(B3): the 2π-propagator integrals are represented by $\mathcal{J}^{\pi\pi},\mathcal{J}_{1,2,3}^{\pi\pi}$ and the one-nucleon–2π-propagator integrals are represented by

$\gamma_{0,1,2,3,4,5}$.[1] For convenience, they are represented by the 14 integrals I_i, $i=1,\ldots,14$ in the one-loop amplitudes (37)–(47). Then using the results of Appendix B 1 and B 2, the integrals and hence the amplitudes are written down as a linear combination of the UV-finite (L-independent) and UV-divergent (L-dependent) terms. In Table I we identify the equation in Appendix B used to evaluate each of the 14 one-loop integrals. The numerical values of the UV-finite parts are also given in Table I, for completeness, so that the calculation can be reconstructed by the reader, or for application of the relevant parts to problems other than DCX.

(a)

$$T_{[a]}=0\qquad(37)$$

because $v\cdot(p_2-p_4)=0$.

(b)

$$T_{[b]}=2(\sqrt{2})^6\frac{g_A^2}{48F^6}[-3I_3+M_\pi^2 I_4-M_\pi^2 I_2]$$

$$=2(\sqrt{2})^6\frac{g_A^2 M_\pi^2}{48F^6}\left[\frac{29}{6}L-\frac{85}{576\pi^2}+\frac{\sqrt{5}}{8\pi^2}\right.$$

$$\left.\times\ln\left(\frac{\sqrt{5}+1}{\sqrt{5}-1}\right)+\frac{29}{192\pi^2}\ln\frac{M_\pi^2}{\mu^2}\right].\qquad(38)$$

---

[1]The notations of [6] and [13], where similar integrals have been evaluated, have been modified for this paper; see Appendix B.

(c)

$$T_{[c]} = \frac{g_A^2(\sqrt{2})^8}{96F_\pi^6}[-6M_\pi^2(-M_\pi^2 I_5 - 3I_6 + M_\pi^2 I_7)$$
$$+ 2(M_\pi^2 I_2 + 3I_3 - M_\pi^2 I_4)]$$
$$= \frac{g_A^2 M_\pi^2(\sqrt{2})^8}{96F_\pi^6}\left[-\frac{41}{3}L - \frac{23}{288\pi^2} - \frac{41\sqrt{5}}{120\pi^2}\ln\left(\frac{\sqrt{5}+1}{\sqrt{5}-1}\right) \right.$$
$$\left. - \frac{25}{48\pi^2}\ln\frac{M_\pi^2}{\mu^2} \right]. \tag{39}$$

(d)

$$T_{[d]} = -\frac{2(\sqrt{2})^6}{3}\frac{1}{128F_\pi^6}[-I_3 - 4M_\pi^2 I_1 + 4M_\pi^3 I_{11}]$$
$$= -\frac{(\sqrt{2})^6}{3}\frac{M_\pi^2}{64F_\pi^6}\left[\frac{55}{6}L - \frac{173}{576\pi^2} + \frac{55}{192\pi^2}\ln\frac{M_\pi^2}{\mu^2} \right.$$
$$\left. + \frac{53\sqrt{5}}{192\pi^2}\ln\left(\frac{\sqrt{5}+1}{\sqrt{5}-1}\right) + \frac{1}{2\pi}\ln\left(\frac{1+\sqrt{5}}{2}\right) \right]. \tag{40}$$

(e)

$$T_{[e]} = -(\sqrt{2})^8\frac{1}{48F_\pi^6}[I_3 + 3M_\pi^2 I_6]$$
$$= \frac{M_\pi^2(\sqrt{2})^8}{48F_\pi^6}\left[\frac{8}{3}L - \frac{1}{96\pi^2}\left(11 - 8\ln\frac{M_\pi^2}{\mu^2}\right) \right.$$
$$\left. + \frac{7\sqrt{5}}{96\pi^2}\ln\left(\frac{\sqrt{5}+1}{\sqrt{5}-1}\right) \right]. \tag{41}$$

(f)

$$T_{[f]} = \frac{2(\sqrt{2})^6}{96F_\pi^6}I_3$$
$$= \frac{(\sqrt{2})^6 M_\pi^2}{48F_\pi^6}\left[-\frac{7}{6}L - \frac{1}{576\pi^2} \right.$$
$$\left. \times\left(-29 + 21\ln\frac{M_\pi^2}{\mu^2}\right) - \frac{5\sqrt{5}}{192\pi^2}\ln\left(\frac{\sqrt{5}+1}{\sqrt{5}-1}\right) \right]. \tag{42}$$

(g)

$$T_{[g]} = -\frac{(\sqrt{2})^6 g_A^2}{576F_\pi^6}\left[\left(-\frac{3}{2}I_8 + 9I_{10}\right)\vec{\sigma}^{(1)}\cdot\vec{P}\vec{\sigma}^{(2)}\cdot\vec{P} \right.$$
$$\left. - 9I_9\vec{\sigma}^{(1)}\cdot\vec{\sigma}^{(2)} \right]. \tag{43}$$

Using

$$I_{10} = \frac{1}{3}I_8; \quad I_9 = -\frac{1}{2}\Delta_\pi(0,M_\pi^2), \tag{44}$$

one gets

$$T_{[g]} = -\frac{(\sqrt{2})^6 g_A^2}{576F_\pi^6}\left[\left(-3L - \frac{3}{32\pi^2} \right.\right.$$
$$\left.\times\left(1 + \ln\frac{M_\pi^2}{\mu^2}\right)\right)\vec{\sigma}^{(1)}\cdot\vec{P}\vec{\sigma}^{(2)}\cdot\vec{P}$$
$$\left. + \left(9M_\pi^2 L + \frac{9M_\pi^2}{32\pi^2}\ln\frac{M_\pi^2}{\mu^2}\right)\vec{\sigma}^{(1)}\cdot\vec{\sigma}^{(2)} \right]. \tag{45}$$

One thus gets

$$\langle S=0|T_{[h]}|S=0\rangle = -\frac{(\sqrt{2})^6 g_A^2}{576F_\pi^2}\left[-24L + \frac{1}{32\pi^2} \right.$$
$$\left.\times\left(3 - 24\ln\frac{M_\pi^2}{\mu^2}\right) \right]. \tag{46}$$

(h)

$$T_{[h]} = 2\times\frac{2(\sqrt{2})^6 g_A^2}{384F_\pi^6}[(-6I_9 - 6M_\pi I_{13})\vec{\sigma}^{(1)}\cdot\vec{\sigma}^{(2)}$$
$$+ (-I_8 - 2M_\pi I_{12} + 6I_{10} + 6M_\pi I_{14})\vec{\sigma}^{(1)}\cdot\vec{P}\vec{\sigma}^{(2)}\cdot\vec{P}]$$
$$= 2\times\frac{2(\sqrt{2})^6 g_A^2}{384F_\pi^6}\left[\left(-6L - \frac{3}{16\pi^2}\ln\frac{M_\pi^2}{\mu^2} + \frac{1}{4\pi^2} \right.\right.$$
$$\left.\times\left[3 - \frac{3\pi^2}{8}\right]\right)M_\pi^2\vec{\sigma}^{(1)}\cdot\vec{\sigma}^{(2)} + \left(-2L - \frac{3}{16\pi^2} \right.$$
$$\left.\left. - \frac{1}{16\pi^2}\ln\frac{M_\pi^2}{\mu^2} + \frac{3}{32}\right)\vec{\sigma}^{(1)}\cdot\vec{P}\vec{\sigma}^{(2)}\cdot\vec{P} \right]. \tag{47}$$

One thus gets

$$\langle S=0|T_{[h]}|S=0\rangle = (\sqrt{2})^6\frac{g_A^2 M_\pi^2}{96F_\pi^6}\left[20L - \frac{1}{16\pi^2}(33 - 3\pi^2) \right.$$
$$\left. + \frac{5}{8\pi^2}\ln\frac{M_\pi^2}{\mu^2} \right]. \tag{48}$$

Finally, the total one-loop contribution to the DCX amplitude is given by

TABLE II. Amplitudes for one-loop graphs.

$\langle S=0|T_{[x]}|S=0\rangle$	UV-finite integral (units of MeV^{-4})	UV-divergent portion $\left(\text{coefficient of } \dfrac{(\sqrt{2})^6 M_\pi^2}{F_\pi^6}\right)L$
a	$-$	$-$
b	-7.7×10^{-10}	$2\times\dfrac{29g_A^2}{288}$
c	10^{-9}	$-2\times\dfrac{41g_A^2}{288}$
d	1×10^{-11}	$-\dfrac{55}{1152}$
e	-2.9×10^{-10}	$\dfrac{1}{9}$
f	7×10^{-11}	$-\dfrac{7}{288}$
g	1.9×10^{-10}	$\dfrac{g_A^{02}}{24}$
h	-10^{-9}	$\dfrac{5g_A^{02}}{24}$
Total	$-(7.9\pm 1.6)\times 10^{-10}$	$\dfrac{1}{24}\times\left(\dfrac{15}{16}+4g_A^2\right)$
	for $\mu=1\pm 0.5$ GeV	

$$\langle S=0|T_{\text{total}}(\text{one-loop})|S=0\rangle=\frac{(\sqrt{2})^6 M_\pi^2}{24F_\pi^6}\left(\left[4g_A^2+\frac{15}{16}\right]L\right.$$

$$+\left[-\frac{181}{256\pi^2}+\frac{3}{64}\right]g_A^2$$

$$-\frac{157}{1536\pi^2}+\frac{1}{64\pi^2}\ln\frac{M_\pi^2}{\mu^2}\left[\frac{15}{8}+5g_A^2\right]+\frac{\sqrt{5}}{24\pi^2}\ln\left(\frac{\sqrt{5}+1}{\sqrt{5}-1}\right)$$

$$\left.\times\left[-\frac{11}{10}g_A^2+\frac{39}{64}\right]-\frac{1}{16\pi}\ln\left[\frac{1+\sqrt{5}}{2}\right]\right). \qquad (49)$$

The numerical values of the UV-finite parts of the one-loop amplitudes and their UV-divergent portions are given in Table II.

Hence, comparing the numerical values of Eq. (27) and Eq. (49) one sees that the one-loop graphs contribute an increase of about a 1.6% relative to the tree graphs, after removal of divergent terms (see Sec. V). This agrees with the expectation that the second-order correction in the chiral expansion should be smaller by a factor of $M_\pi^2/(4\pi F_\pi)^2$ ≈ 0.014 than the leading order. The suppression of the two-nucleon graphs relative to the leading order tree graphs can be seen explicitly by comparing expressions (27) and (49). (This is in contrast to the large one-loop corrections for the π-π and π-N vertices, which are discussed in Sec. VI.) Also note the relative insensitivity of the total (finite) one-loop amplitude to the choice of the renormalization point μ, as shown in the last line of Table II; a 50% change in μ gives a 20% change in amplitude.

From Table II, one sees that the dominant one-loop contributions come from graphs (b), (c), and (h). This is probably related to the following observations. First, as is clear from Table I, the one-nucleon–2π-propagator loop integrals dominate over the 2π-propagator integrals.[2] Second, graphs (b), (c), and (h) are proportional to $g_A^2>1$, as compared to graphs (d), (e), and (f) (which do not have a g_A^2 dependence).

V. RENORMALIZATION BY CONTACT TERMS

In this section we discuss the renormalization of the one-loop graphs evaluated in Sec. IV. To remove the UV divergence in $(3+1)$-dimensional space, one has to look for terms whose contributions precisely cancel the coefficient of the ''L'' in the (two-nucleon) one-loop amplitudes. Given the structure of the UV-divergent parts of the one-loop amplitudes, 2π–two-nucleon contact terms (Fig. 5) of $\mathcal{O}(q^2)$ should do the job as the correct counter terms, as will become clear from Eqs. (51) and (52) below.

The contact terms are defined by

$$\lim_{x\to y}\langle\alpha'|\bar{\text{H}}\mathcal{O}_1\text{H}(x)|\alpha\rangle\langle\beta'|\bar{\text{H}}\mathcal{O}_2\text{H}(y)|\beta\rangle, \qquad (50)$$

---

[2]Graph (d) also has a one-nucleon–2π-propagator structure, but the corresponding loop integrals occur in such a way in the amplitude that there is large cancellation between the contributions of $I_k,k=1,3,11$.

with $\alpha \equiv p, I_3$. From the expressions for the amplitudes for the eight one-loop graphs in Sec. IV, before setting $\vec{P}^2 = q_1 \cdot q_2 = M_\pi^2$, one can show that the UV-divergent terms have the following structures [omitting the overall isospin factor $\tau_+^{(1)} \tau_+^{(2)}$ from Eq. (51)]

$$(\vec{P}^2 \text{ or } q_1 \cdot q_2 \text{ or } M_\pi^2) \times \mathbf{1},$$

$$(\vec{P}^2 \text{ or } q_1 \cdot q_2 \text{ or } M_\pi^2) \times \vec{\sigma}^{(1)} \cdot \vec{\sigma}^{(2)}, \qquad (51)$$

$$\vec{\sigma}^{(1)} \cdot \vec{P} \vec{\sigma}^{(2)} \cdot \vec{P}.$$

On taking the Fourier transform of the amplitudes (51), one gets the local forms:

$$\sim (M_\pi^2, q_1 \cdot q_2, \partial_i^1 \partial_j^2) \delta^{(3)}(\vec{x}_1 - \vec{x}_2) \equiv O(q^2). \qquad (52)$$

Thus one requires $O(q^2, \phi^2)$ 2 2π–2-nucleon contact terms with $\tau_+^{(1)} \tau_+^{(2)}$ isospin structure.

For the purpose of renormalization, one needs to consider nine 2π–two-nucleon contact terms, written in terms of

$$u_\mu, \overset{\leftarrow+\rightarrow}{D_\mu}, \chi_+, \text{ and } \phi, \qquad (53)$$

$[\overset{\leftarrow+\rightarrow}{D_\mu} \equiv (\partial_\mu + \Gamma_\mu) + (\overset{\leftarrow}{\partial} - \Gamma_\mu); \ \chi_+ = M^2(U + U^\dagger)]$. The finite parts of these nine terms will not contribute, as explained later in this section.

One needs to include at least ϕ explicitly as a building block for DCX for the following reason. The ϕ in Eq. (A2) can be expanded in terms of the generators of the nucleon isospin group as

$$\phi = \tau_3 \phi^0 + \sqrt{2}(\tau_+ \phi^- + \tau_- \phi^+), \qquad (54)$$

where $\tau_\pm = \frac{1}{2}(\tau_1 \pm i\tau_2)$, and ϕ^+ either annihilates π^- or creates π^+, and ϕ^- either annihilates π^+ or creates π^-. In DCX, a π^+ goes over to π^-, implying that one requires $\mathcal{O}_1(x)$ and $\mathcal{O}_2(y)$ in Eq. (50) to consist at least of $\phi_-(x)\phi_-(y)$ (or derivatives thereof), or in terms of the isospin generators, $\tau_+^{(1)}\tau_+^{(2)}$, where the superscripts refer to nucleons 1 and 2. Further, using Table III one can construct Table IV for $\mathcal{O}_1(x)\mathcal{O}_2(y)$ relevant to DCX (again omitting $\tau_+^{(1)}\tau_+^{(2)}$) which has to include terms of the type isovector $\times$ isovector.

Note that $S \cdot u(x) S \cdot u(y)$ will not contribute in the static limit and at threshold [use Eq. (16) and $v_{1,2}^\mu = (1, \vec{0})$]. The relevant counter terms are listed below:

$$\lim_{x \to y} \left[\frac{\alpha_1}{F_\pi^4} \bar{H}(x) \frac{\phi(x)}{F_\pi} H(x) \bar{H}(y) \frac{\phi(y)}{F_\pi} H(y) \langle \chi_+(x) \rangle \right.$$

$$+ \frac{\alpha_2}{F_\pi^4} \bar{H}(x) u_\mu(x) H(x) \bar{H}(y) u^\mu(y) H(y) \frac{\alpha_3}{F_\pi^4} \bar{H}(x) v \cdot u(x) H(x) \bar{H}(y) v \cdot u(y) H(y)$$

$$\times \frac{\alpha_4}{F_\pi^4} \bar{H}(x) \frac{\phi(x)}{F_\pi} \overset{\leftarrow+\rightarrow}{D^\mu}(x) H(x) \bar{H}(y) \frac{\phi(y)}{F_\pi} \overset{\leftarrow+\rightarrow}{D_\mu}(y) H(y) + \frac{\alpha_5}{F_\pi^4} \bar{H}(x) \frac{\phi(x)}{F_\pi} S_\mu^{(1)} H(x) \bar{H}(y) \frac{\phi(y)}{F_\pi} S^{(2),\mu} H(y) \langle \chi_+(x) \rangle$$

$$+ \frac{\alpha_6}{F_\pi^4} \bar{H}(x) u_\mu(x) S_\nu^{(1)} H(x) \bar{H}(y) u^\mu(y) S^{(2),\nu} H(y) + \frac{\alpha_7}{F_\pi^4} \bar{H}(x) v \cdot u S^{\mu,(1)} H(x) \bar{H}(y) v \cdot u(y) S_\mu^{(2)} H(y)$$

$$+ \frac{\alpha_8}{F_\pi^4} \bar{H}(x) S_\mu^{(1)} \frac{\phi(x)}{F_\pi} \overset{\leftarrow+\rightarrow}{D^\nu}(x) H(x) \bar{H}(y) S^{(2),\mu} \frac{\phi(y)}{F_\pi} \overset{\leftarrow+\rightarrow}{D_\nu}(y) H(y) + \frac{\alpha_9}{F_\pi^4} \bar{H}(x) \frac{\phi(x)}{F_\pi} S^{(1)} \cdot \overset{\leftarrow+\rightarrow}{D_\nu}(x) H(x)$$

$$\times \bar{H}(y) \frac{\phi(y)}{F_\pi} S^{(2)} \cdot \overset{\leftarrow+\rightarrow}{D}(y) H(y) \Bigg]. \qquad (55)$$

The coupling constants $\{\alpha_i\}$ have been made dimensionless by construction of the terms.

It should be noted that the following five types of UV-finite 2π–two-nucleon $O(q^2)$ contact terms will also contribute to off-threshold DCX:

$$\lim_{x \to y} [\epsilon^{\mu\nu\rho\lambda} v_\rho \bar{H}(x) u_\mu(x) H(x) \bar{H}(y) S_\nu^{(2)} u_\lambda(y) H(y),$$

$$\epsilon^{\mu\nu\rho\lambda} v_\rho \bar{H}(x) u_\mu(x) H(x) \bar{H}(y) \phi(y) S_\nu^{(2)} D_\lambda H(y),$$

$$\epsilon^{\mu\nu\rho\lambda} v_\rho \bar{H}(x) S_\nu^{(1)} u_\mu(x) H(x) \bar{H}(y) \phi(y) D_\lambda H(y),$$

$$\epsilon^{\mu\nu\rho\lambda} v_\rho \bar{H}(x) u_\mu D_\lambda S_\nu^{(1)} H(x) \bar{H}(y) \phi(y) H(y),$$

$$\epsilon^{\mu\nu\rho\lambda} v_\rho \bar{H}(x) u_\mu(x) D_\lambda H(x) \bar{H} \phi(y) S_\nu^{(2)} H(y)]. \qquad (56)$$

By renormalization of loop-graph integrals, one gets a constraint on a linear combination of the UV-divergent parts of LECs of seven of the nine 2π–two-nucleon contact

counter terms of Eq. (55). First one calculates the amplitudes T corresponding to the contact terms of Eq. (55). Then, writing $\alpha_i = \alpha_i^r + \lambda_i L$ [where L was defined in Eq. (36)], and comparing with the UV-divergent portion of the total one-loop amplitude (49) and Table II, one gets the following conditions [suppressing the two pairs of Pauli spinors and using Eqs. (15)–(17)]:

(1) spin-independent renormalization (graphs [(a)+⋯+(f)]):

$$(\sqrt{2})^2(4\lambda_1 + 2\lambda_2 - 2\lambda_3) = (\sqrt{2})^6\left(-\frac{g_A^2}{12} - \frac{5}{128}\right), \quad (57)$$

(2) spin-dependent renormalization (graphs [(g)+(h)]):

$$(\sqrt{2})^2\left(3\lambda_5 + \frac{3}{2}\lambda_6 + 6\lambda_7 - 2\lambda_9\right) = -(\sqrt{2})^6\frac{g_A^2}{4}, \quad (58)$$

which on addition gives

$$(\sqrt{2})^2\left(4\lambda_1 + 2\lambda_2 - 2\lambda_3 + 3\lambda_5 + \frac{3}{2}\lambda_6 + 6\lambda_7 - 2\lambda_9\right)$$
$$= -\frac{(\sqrt{2})^6}{24}\left(\frac{15}{16} + 4g_A^2\right). \quad (59)$$

Note that the λ_4, λ_8 terms do not contribute at the kinematic point (17). So, it is clear that the renormalization of the loop integrals can be accomplished by the 2π–two-nucleon contact terms.

Because the nucleon-nucleon interaction has a strong short range repulsion, the nucleon-nucleon wave function vanishes at short relative distances. Since the contact terms in Eqs. (55) and (56) behave as $\delta^{(3)}(\vec{x} - \vec{y})$, one does not get any contribution from these 2π–two-nucleon contact terms, as well as from the UV-divergent parts of the one-loop integrals. Hence, only UV-finite parts of the loop integrals contribute to the DCX loop amplitudes after renormalization.

VI. SUMMARY AND DISCUSSION

The goal of this paper has been to calculate the one-loop correction to the two-nucleon amplitudes for pion double charge exchange (DCX) scattering by a nuclear target, at threshold, in the framework of HBChPT. For a numerical estimate of the two-nucleon–one-loop correction, the amplitudes are evaluated at a typical kinematic point (17). These are compared to the leading order amplitudes (for the tree graphs), obtained in the same theoretical framework.

TABLE III. Properties of building blocks.

Building block	Isospin nature	Chiral order
D_μ	isoscalar($\equiv \partial_\mu$) $+$ isovector($\equiv \Gamma_\mu$)	$O(q)$
u_μ	isovector	$O(q)$
χ_+	isoscalar	$O(q^2)$
ϕ	isovector	$O(1)$

The two-nucleon–one-loop graphs give a threshold contribution of about 0.016 relative to the leading order tree graphs at the same kinematics [with $(\vec{p}' - \vec{p})^2 = M_\pi^2$]. Both calculations are done in the static limit and the impulse approximation for the nucleons, and using the renormalized values of the axial-vector coupling, pion-decay constants, and the pion and nucleon masses. As noted at the end of Sec. V, these corrections are of the order of $M_\pi^2/(4\pi F_\pi)^2 \simeq 0.014$ times the tree graphs in LO ($\nu = 0$). This is as expected for a chiral correction of $\nu = 2$.

As noted in Sec. II, there are also corrections to the LO tree graphs to order $\nu = 2$ arising from corrections to the π-π and π-N vertices, which have been studied in the literature. The π-π vertex has been determined to the required order (to one loop) [3], with the LECs fixed phenomenologically. However, although the π-N vertex corrections have also been studied through one loop [4,11], the LECs have only been determined for the on-shell threshold cases of π-N scattering lengths [4] and $\pi^\pm$ production on a single nucleon [11]. Therefore, there is not enough information from these studies to fix all the vertex LECs required to carry out the full $\nu = 2$ calculation of the DCX tree graphs.

However, the one-loop calculations cited do show large corrections to the vertices. We can estimate how much this would change the DCX tree-graph amplitudes by using the on-shell results as follows. First, we characterize the three amplitudes of Eqs. (21), (23), and (25) in terms of vertex coefficients:

$$T_{[a]} \sim D_1 g_A,$$
$$T_{[b]} \sim A g_A^2, \quad (60)$$
$$T_{[c]} \sim (a^-)^2.$$

The amplitude D_1 is the $\pi N \to \pi \pi N$ threshold amplitude [11] that contributes to the DCX tree graph [a]. To leading order, $D_1(LO) \sim g_A/F_\pi^2$. The corrections through one loop give [11]

$$D_1 = D_1(LO)(1 + 0.67). \quad (61)$$

The loop correction is actually 0.15; the larger correction, 0.52, is from a ''recoil'' term of order M_π^2/m.

TABLE IV. $\mathcal{O}_1(x)\mathcal{O}_2(y)$ relevant to DCX.

Momentum-spin form	Coordinate-spin operators
$M_\pi^2 \times \mathbf{1}$	$\phi(x)\phi(y)\langle\chi_+(x)\rangle$
$q_1 \cdot q_2 \times \mathbf{1}$	$u_\mu(x)u^\mu(y)$; $v \cdot u(x) v \cdot u(y)$
$\vec{P}^2 \times \mathbf{1}$	$\phi(x) \overset{\leftarrow+\rightarrow}{D_\mu}(x)\phi(y)\overset{\leftarrow+\rightarrow}{D^\mu}(y)$
$M_\pi^2 \times \vec{\sigma}^{(1)} \cdot \vec{\sigma}^{(2)}$	$S_\mu^{(1)}\phi(x)S^{(2),\mu}\phi(y)\langle\chi_+\rangle$
$q_1 \cdot q_2 \times \vec{\sigma}^{(1)} \cdot \vec{\sigma}^{(2)}$	$u_\mu(x)S_\nu^{(1)}u^\mu S^{\nu,(2)}$; $v \cdot u(x)S^{\mu,(1)} v \cdot u(y)S_\mu^{(2)}$
$\vec{P}^2 \times \vec{\sigma}^{(1)} \cdot \vec{\sigma}^{(2)}$	$\phi(x)S^{(1),\mu}\overset{\leftarrow+\rightarrow}{D_\nu}(x)\phi(y)S_\mu^{(2)}\overset{\leftarrow+\rightarrow}{D^\nu}(y)$
$\vec{\sigma}^{(1)} \cdot \vec{P}\vec{\sigma}^{(2)} \cdot \vec{P}$	$\phi(x)S^{(1)} \cdot \overset{\leftarrow+\rightarrow}{D}(x)\phi(y)S^{(2)} \cdot \overset{\leftarrow+\rightarrow}{D}(y)$

The amplitude A gives the DCX contribution to tree graph [b] from the π-π vertex, and can easily be shown to be to the two s-wave scattering lengths a_I, with isospins $I=0,2$, by

$$A=(2a_0+a_2)/3. \tag{62}$$

To LO, $A(\text{LO})\sim M_\pi/F_\pi^2$. The one-loop corrections [3] change this to

$$A=A(\text{LO})(1+0.30). \tag{63}$$

The isovector πN scattering length a^- contributes to the double-scattering tree graph [c]. To LO, $a^-(\text{LO})$ $\sim M_\pi/F_\pi^2$. With corrections through one-loop, this becomes [4]

$$a^-=a^-(\text{LO})(1+0.046). \tag{64}$$

This small correction masks a 20% contribution of the loop, partially cancelled by the ''recoil'' correction.

If we now use these corrected values for the vertices in the expressions (60), we obtain the following estimates of their effect to order $\nu=2$ on the tree-graph amplitudes:

$$T_{[a]}=1.67 \ T_{[a]}(\text{LO}),$$

$$T_{[b]}=1.30 \ T_{[b]}(\text{LO}), \tag{65}$$

$$T_{[c]}=1.092 \ T_{[c]}(\text{LO}).$$

These corrections are much larger than the one-loop corrections of this paper, which involve both nucleons participating in the DCX reaction. However, the vertex corrections are only estimates, since not all the off-shell vertex coefficients are determined.

So we are led to two conclusions about corrections to DCX to order $\nu=2$. First, the one-loop correction to the tree graph amplitudes is small, whether compared to the LO tree amplitudes, or to those amplitudes also corrected to one-loop order. The dominant contributions [graphs 3(b), 3(c), and 4(h)] all have one nucleon propagator, and are proportional to $g_A^2>1$. The largest, 4(h), is clearly a correction to the largest tree graph, 2(c), for double scattering. (Triple scattering on two nucleons has not been included; it belongs with other triple scattering graphs on three nucleons.) The result is weakly dependent on the choice of the renormalization point μ.

For the purpose of renormalization of the loop graphs, we found that nine 2π–two-nucleon contact terms are required, of which seven contribute at the specific kinematic point considered (17). However, since we have assumed that the nuclear wave functions vanish near zero (relative) distance of nucleon separation, none of the (UV-finite parts) of the contact terms will contribute, because of the $\delta^{(3)}(\vec{x}-\vec{y})$ in the forms of contact terms of Eqs. (55) and (56). If this anticorrelation assumption were relaxed, then one would have nine unknown LECs for Eq. (55) [seven for the kinematic point (17)], and five for Eq. (56), to be determined empirically, to the order considered $[O(q^2)]$.

The second conclusion is that the one-loop corrections to the π-π and π-N vertices produce the largest corrections at order $\nu=2$ to the LO tree amplitudes. The large correction to the π-π vertex has been related to the pion radius [3], that is, to the correction for the LO assumption of a point pion. Presumably, similar effects, including resonant contributions, give the large π-N vertex corrections. It is clear that these corrections are anomalously large, while the one-loop corrections to the two-nucleon amplitudes are of expected size for the $O(q^2)$ terms. The latter may reflect the fact that the N-N system is already of finite size.

However, as noted above, the vertex corrections for the π-N amplitudes have not been fixed sufficiently for a complete calculation of the DCX tree amplitudes. This would require an extension of the one-loop theory of the various π-N amplitudes to off-shell kinematics, beyond what has already been done in the literature. As a practical matter, the π-N on-shell constants could be taken directly from experiment, as in the impulse approximation, rather than from higher orders in chiral perturbation theory.

APPENDIX A: VERTICES AND F's FOR ONE-LOOP GRAPHS FOR π-NN

The pion field is represented as a matrix-valued SU(2) field U defined as following:

$$e^{i(\phi/F_\pi)}\equiv U(\pi), \tag{A1}$$

where ϕ is a traceless (as det $U=1$) matrix written in terms of the pion triplet as

$$\sqrt{2}\begin{pmatrix} \dfrac{\pi^0}{\sqrt{2}} & \pi^+ \\ \pi^- & -\dfrac{\pi^0}{\sqrt{2}} \end{pmatrix}. \tag{A2}$$

The matrix is written in a space that corresponds to the standard (p/n) isospinors which are implied in the H notation.

1. Vertices

The leading order terms in (H)ChPT, written using Eqs. (A1) and (A2), that are used for the evaluation of $m\pi$-$\bar{N}N(m=1,2,3,4)$ and 4-π vertices, are written out:

$$1\,\pi\bar{N}N : g_A\bar{H}S\cdot u^{(1)}H = -(\sqrt{2})\frac{g_A}{F_\pi}\left[\frac{1}{\sqrt{2}}\bar{p}S\cdot\partial\pi^0 p + \bar{p}S\cdot\partial\pi^+ n + \bar{n}S\cdot\partial\pi^- n - \frac{1}{\sqrt{2}}\bar{n}S\cdot\partial\pi^0 n\right],$$

$$2\,\pi\bar{N}N : i\bar{H}v\cdot D^{(2)}H \equiv \bar{H}v\cdot\Gamma^{(2)}H = (\sqrt{2})^2\frac{i}{8F_\pi^2}[\bar{p}p\,\pi^{[+}v\cdot\partial\pi^{-]} + \sqrt{2}\bar{p}n\,\pi^{[0}v\cdot\partial\pi^{+]} + \sqrt{2}\bar{n}p\,\pi^{[-}v\cdot\partial\pi^{0]} + \bar{n}n\,\pi^{[-}v\cdot\partial\pi^{+]}],$$

$$3\,\pi\bar{N}N : g_A\bar{H}S\cdot u^{(3)}H = (\sqrt{2})^3\frac{g_A^2}{12F_\pi^3}\left[\frac{1}{\sqrt{2}}\bar{p}[2\pi^+\pi^- S\cdot\partial\cdot\pi^0 - \pi^0(\pi^+ S\cdot\partial\pi^- + \pi^- S\cdot\partial\pi^+)]p + \bar{p}(\pi^{02}S\cdot\partial\pi^+ - \pi^+\pi^0 S\cdot\partial\pi^0\right.$$

$$+ \pi^+\pi^{[-}S\cdot\partial\pi^{+]})n$$

$$\left.+ \text{H.c.} + \frac{1}{\sqrt{2}}\bar{n}[-2\pi^+\pi^- S\cdot\partial\pi^0 + \pi^0 + \pi^0(\pi^- S\cdot\partial\pi^+ + \pi^+ S\cdot\partial\pi^-)]n\right],$$

$$4\,\pi\bar{N}N : \bar{H}iv\cdot D^{(4)}H \equiv \bar{H}iv\cdot\Gamma^{(4)}H(\sqrt{2})^4\frac{i}{96F_\pi^4}\left(\frac{\pi^{02}}{2}+\pi^+\pi^-\right)[\bar{p}p\,\pi^{[-}v\cdot\partial\pi^{+]} + (\sqrt{2}\bar{p}n\,\pi^{[+}v\cdot\partial\pi^{0]} + \text{H.c.}) + \bar{n}n\,\pi^{[+}v\cdot\partial\pi^{-]}],$$

$$4\,\pi : \frac{F_\pi^2}{4}[\langle\partial^\mu U^\dagger\partial_\mu U\rangle + M_\pi^2\langle(U^\dagger + U - 2)\rangle]^{(4)} = (\sqrt{2})^4\frac{1}{24F_\pi^2}[-2\pi^+\pi^-\partial_\mu\pi^+\partial^\mu\pi^- + (\pi^-)^2(\partial_\mu\pi^+)^2 + (\pi^+)^2(\partial_\mu\pi^-)^2$$

$$+ M_\pi^2(\pi^+)^2(\pi^-)^2]. \tag{A3}$$

2. Combinatoric factors for one-loop graphs

The combinatoric factors ''f'' of Eq. (19) for one-loop graphs, are evaluated. First, $S^{(n)}$ [see Eq. (19)] is written out in terms of ''$\bar{H}\phi^m H$,'' $m=1,2,3,4$ and ''ϕ^4,'' which represent the $m\pi - n_i$ nucleon vertices with $m=1,2,3,4; n_i=2$ and $m=4; n_i=0$. Then, using the time ordering properties of bosonic and fermionic bilinear fields, those terms relevant to the DCX one-loop graphs are picked out. Then on comparison with Eq. (19), the combinatoric factors are read off for the eight two-nucleon one-loop graphs. They are listed along with the corresponding forms of Eq. (19) in Table V.

APPENDIX B: ONE-LOOP INTEGRALS

There are 11 one-loop integrals defined and evaluated in this appendix. The integrals $\gamma_{4,6}$ do not occur in the one-loop DCX amplitudes as discussed later. The notations used, though similar to the ones used by [6] and [13], are slightly different.

Four of those integrals are referred to as basic integrals: $\Delta_\pi(0,M^2)$, $J^{\pi N}$, $\mathcal{J}^{\pi\pi}, \gamma_0$, evaluated at different kinematic points. [The 0 in $\Delta_\pi(0,M^2)$ implies that the ''external'' four-momentum squared ''$\mathcal{P}^2$'' that appears in other integrals, is zero.] They are defined below:

$$\frac{1}{i}\int\frac{d^dk}{(2\pi)^d}\frac{1}{M^2 - k^2 - i\epsilon} \equiv \Delta_\pi(0,M^2),$$

$$\frac{1}{i}\int\frac{d^dk}{(2\pi)^d}\frac{1}{(v\cdot k - \omega - i\epsilon)(M_\pi^2 - k^2 - i\epsilon)} \equiv J^{\pi N}(\omega),$$

$$\frac{1}{i}\int\frac{d^dk}{(2\pi)^d}\frac{1}{(M^2 - k^2 - i\epsilon)(M_\pi^2 - (k-\mathcal{P})^2 - i\epsilon)} \equiv \mathcal{J}^{\pi\pi}(\mathcal{P}^2;M^2),$$

$$\frac{1}{i}\int\frac{d^dk}{(2\pi)^d}\frac{1}{(v\cdot k - \omega - i\epsilon)(M^2 - k^2 - i\epsilon)(M^2 - (k-\mathcal{P})^2 - i\epsilon)} \equiv \gamma_0(\omega,\Omega,\mathcal{P}^2), \tag{B1}$$

TABLE V. Combinatoric factors for the one-loop graphs.

x	$S^{(n)}_{[x]} = \dfrac{i^n}{n!} \int \Pi^n_{k=1} d^4 x_k$ $\mathcal{T}[\Pi^n_{i=1} \Sigma_j \mathcal{L}^I_j(x_i)]$	$f i^n \int \Pi^n_{k=1} d^4 x_k$ $\mathcal{T}[\Pi^n_{i=1} \mathcal{L}^I_i(x_i)]$ relevant to x	f
a	–	–	–
b	$\dfrac{i^3}{6} \int \Pi^3_{i=1} d^4 x_i \mathcal{T}[\Pi^3_{i=1}$ $[\bar{H}(\phi + \phi^2 + \phi^3)H](x_i)]$	$i^3 \Pi^3_{i=1} \int d^4 x_i$ $\mathcal{T}[(\bar{H}\phi H)(x_1)(\bar{H}\phi^2 H)(x_2)$ $(\bar{H}\phi^3 H)(x_3)]$	1
c	$\dfrac{i^4}{24} \Pi^4_{i=1} \int d^4 x_i \mathcal{T}[\Pi^4_{i=1}[\bar{H}(\phi + \phi^2)H$ $+ \phi^4](x_i)]$	$\dfrac{1}{2} \Pi^4_{i=1} \int d^4 x_i T[(\bar{H}\phi H)(x_1)(\bar{H}\phi H)(x_2)$ $(\bar{H}\phi^2 H)(x_3)\phi^4(x_4)]$	$\dfrac{1}{2}$
d	$\dfrac{i^3}{6} \Pi^3_{i=1} \int d^4 x_i \mathcal{T}[(\bar{H}\phi^2 H)(x_1)$ $(\bar{H}\phi^2 H)(x_2)(\bar{H}\phi^2 H)(x_3)]$	$\dfrac{i^3}{6} \Pi^3_{i=1} \int d^4 x_i \mathcal{T}[(\bar{H}\phi^2 H)(x_1)$ $(\bar{H}\phi^2 H)(x_2)(\bar{H}\phi^2 H)(x_3)]$	$\dfrac{1}{6}$
e	$\dfrac{i^3}{6} \int \Pi^3_{i=1} d^4 x_i \mathcal{T}[\Pi^3_{i=1}(\bar{H}\phi^2 H + \phi^4)(x_i)]$	$\dfrac{i^3}{2} \Pi^3_{i=1} \int d^4 x_i \mathcal{T}[(\bar{H}\phi^2 H)(x_1)$ $(\bar{H}\phi^2 H)(x_2)\phi^4(x_3)]$	$\dfrac{1}{2}$
f	$\dfrac{i^2}{2} \Pi^2_{i=1} \int d^4 x_i \mathcal{T}[[\bar{H}(\phi^2 + \phi^4)H](x_1)$ $[\bar{H}(\phi^2 + \phi^4)H](x_2)]$	$i^2 \Pi^4_{i=1} \int d^4 x_i \mathcal{T}[(\bar{H}\phi^2 H)(x_1)$ $(\bar{H}\phi^4 H)(x_2)]$	1
g	$\dfrac{i^2}{2} \Pi^2_{i=1} \int d^4 x_i \mathcal{T}[(\bar{H}\phi^3 H)(x_1)$ $(\bar{H}\phi^3 H)(x_2)]$	$\dfrac{i^2}{2} \Pi^2_{i=1} \int d^4 x_i \mathcal{T}[(\bar{H}\phi^3 H)(x_1)$ $(\bar{H}\phi^3 H)(x_2)]$	$\dfrac{1}{2}$
h	$\dfrac{i^3}{6} \int \Pi^3_{i=1} d^4 x_i \mathcal{T}[\Pi^3_{i=1}$ $\bar{H}(\phi + \phi^2 + \phi^3)H](x_i)$	$i^3 \int d^4 x_1 \int d^4 x_2 \int d^4 x_3 T[(\bar{H}\phi H)(x_1)$ $(\bar{H}\phi^2 H)(x_2)(\bar{H}\phi^3 H)(x_3)]$	1

with $\Omega \equiv v \cdot \mathcal{P}$. In [13], $\mathcal{P}^2$ that figures in $\mathcal{J}^{\pi\pi}(\mathcal{P}^2, M^2)$ is ≥ 0. In this paper, one requires $\mathcal{P}^2 \leq 0$.

The integrals $\Delta_\pi(0, M^2)$, $\mathcal{J}^{\pi\pi}(\mathcal{P}^2; M^2)$ and $J^{\pi N}(\omega)$ have already been evaluated in the literature [6,13], where they were denoted by $\Delta_\pi(0)$, $J(s \text{ or } t)$ and $J_0(\omega)$, respectively. We have altered the notation for Δ_π and J to introduce M^2 as a variable, because we need to differentiate these expressions with respect to M^2, as in Eqs. (B11) and (B20). The form of $\gamma_0(\omega, \Omega, \mathcal{P}^2)$, required for DCX, has not been evaluated previously. It is a generalization of the integral denoted by $\gamma_0(\omega)$ in [6], for which $\omega = 0$, $\mathcal{P}^2 = 0$, $\mathcal{P} \rightarrow -\mathcal{P}$ (Ω used in this paper is denoted by ''ω'' in [6]). The reason for introducing Ω and $\mathcal{P}^2$ in addition to ω in the argument of γ_0 becomes clear from the points (a) and (b) in the paragraph after Eq. (B3). Also, note that the indexing $(i = 1, 2, \dots)$ of $\mathcal{J}^{\pi\pi}_i(\mathcal{P}^2; M^2)$ and $\gamma_i(\omega, \Omega, \mathcal{P}^2)$ in Eqs. (B2) and (B3) below differs from that used for the corresponding integrals $J^{\pi\pi}_{2i}(s \text{ or } t)$ and $\gamma_i(\omega)$ in [6,13].

The above four integrals are referred to as ''basic'' because the integrands have no momentum dependence in their numerators, and are the most basic of 1π propagator, one-nucleon–1π propagators, 2π propagators, and one-nucleon–2π propagators integrals, respectively.

The remaining integrals have momentum dependence in numerators (and hence have a tensorial character), and are defined as

$$\frac{1}{i} \int \frac{d^d k}{(2\pi)^d} \frac{k_\mu \text{ or } k_\mu k_\nu}{(M^2 - k^2 - i\epsilon)(M^2_\pi - (k - \mathcal{P})^2 - i\epsilon)}$$

$$\equiv \mathcal{P}_\mu \mathcal{J}^{\pi\pi}_1(\mathcal{P}^2; M^2),$$

$$\text{or } g_{\mu\nu} \mathcal{J}^{\pi\pi}_2(\mathcal{P}^2; M^2) + \mathcal{P}_\mu \mathcal{P}_\nu \mathcal{J}^{\pi\pi}_3(\mathcal{P}^2; M^2), \quad \text{(B2)}$$

$$\frac{1}{i} \int \frac{d^d k}{(2\pi)^d}$$

$$\times \frac{k_\mu \text{ or } k_\mu k_\nu}{(v \cdot k - \omega - i\epsilon)(M^2 - k^2 - i\epsilon)(M^2 - (k - \mathcal{P})^2 - i\epsilon)}$$
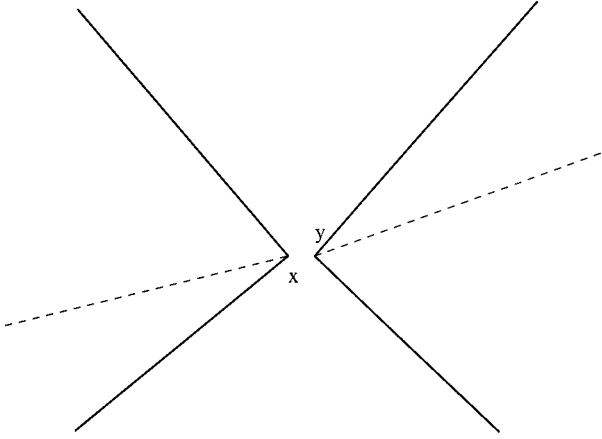
$$\equiv v_\mu \gamma_1(\omega, \Omega, \mathcal{P}^2) + \mathcal{P}_\mu \gamma_2(\omega, \Omega, \mathcal{P}^2),$$

$$\text{or } g_{\mu\nu} \gamma_3(\omega, \Omega, \mathcal{P}^2) + v_\mu v_\nu \gamma_4(\omega, \Omega, \mathcal{P}^2) + \mathcal{P}_\mu \mathcal{P}_\nu \gamma_5$$

$$\times (\omega, \Omega, \mathcal{P}^2) + (v_\mu \mathcal{P}_\nu + v_\nu \mathcal{P}_\mu) \gamma_6(\omega, \Omega, \mathcal{P}^2),$$

$$\text{(B3)}$$

where alternative numerators in k_μ or $k_\mu k_\nu$ have been shown in each case.

Other than notational differences, there are also the following kinematical differences between the integrals of Eq. (B3) and those figuring in [6]: (a) Our $\mathcal{P}^2$ does not vanish, in general, unlike the case for [6], in which $\mathcal{P}^2$ is the four-

$$\frac{1}{i}\int\frac{d^dk}{(2\pi)^d}\frac{f(k_\mu)}{(M_\pi^2-k^2-i\epsilon)^2(M_\pi^2-(k-\mathcal{P})^2-i\epsilon)}, \quad (B4)$$

which can rewritten as

$$-\frac{\partial}{\partial M^2}\frac{1}{i}\int\frac{d^dk}{(2\pi)^d}\frac{f(k_\mu)}{(M^2-k^2-i\epsilon)(M_\pi^2-(k-\mathcal{P})^2-i\epsilon)}, \quad (B5)$$

where M^2 is set equal to M_π^2 after differentiation.

(b) Use is also made of some identities involving the loop integrals, which are valid only in the static limit and impulse approximation (16):

$$\gamma_0(\omega=\pm M_\pi,\Omega=\pm M_\pi,\mathcal{P}^2=(p_4-p_2\pm q_{1,2})^2)$$
$$=\gamma_0(\omega=0,\Omega=\mp M_\pi,\mathcal{P}^2=(p_2-p_4\mp q_{1,2})^2)$$
$$=\gamma_0(\omega=0,\Omega=\mp M_\pi,\mathcal{P}^2=(p_4-p_2\mp q_{1,2})^2)$$
$$=\gamma_0(\omega=\pm M_\pi,\Omega=\pm M_\pi,\mathcal{P}^2=(p_2-p_4\pm q_{1,2})^2),$$
$$(B6)$$

where $p_2^\mu\approx(0,-\vec{p})$, $p_4^\mu\approx(0,-\vec{p}')$, $v^\mu=(1,\vec{0})$, $v\cdot S^{1,2}=0$.

We also use the following the identity:

$$\gamma_0(\omega=\pm M_\pi,\Omega=\pm M_\pi,\mathcal{P}^2=M_\pi^2-\vec{P}^2)$$
$$=\gamma_0(\omega=0,\Omega=\mp M_\pi,\mathcal{P}^2=M_\pi^2-\vec{P}^2). \quad (B7)$$

1. Basic integrals

momentum squared of an on-shell photon; (b) $\omega\neq0;\Omega\equiv v\cdot\mathcal{P}\neq\omega$; (c) we consider $(k-\mathcal{P})^2$ instead of $(k+\mathcal{P})^2$ in the integrals.

Of the nine, two do not contribute to DCX: $\gamma_{4,6}$. The reason is that because these two integrals can occur only in graphs (g) and (h) with integrands having numerators of the type $S^{(1)}\cdot k S^{(2)}\cdot k$, their coefficients will have at least one $S^{(1),(2)}\cdot v$, which vanishes in the static limit. [That is because in the static limit $v^\mu=(1,\vec{0})$ and $S^\mu=(0,\vec{\sigma}/2)$.] The remaining seven can be rewritten as linear combinations of the four basic integrals of Eq. (B1).

All the integrals for the calculation are real, and hence so are all the one-loop amplitudes. This is because the elastic scattering amplitude becomes real at threshold.

Two further simplifications of the calculation are obtained by the following.

(a) The 3π-propagator integrals that occur in the one-loop graph, Fig. 4(e), using Eq. (16), are of the type

The results after evaluation of the basic integrals of Eq. (B1) are given below:

$$\Delta_\pi(0,M^2)=2M^2L+\frac{M^2}{16\pi^2}\ln\frac{M^2}{\mu^2}+\mathcal{O}(d-4),$$

$$J^{\pi N}(\omega)=-4L\omega+\frac{\omega}{8\pi^2}\left(1-\ln\frac{M_\pi^2}{\mu^2}\right)-\frac{1}{4\pi^2}\sqrt{M_\pi^2-\omega^2}\arccos\left(-\frac{\omega}{M_\pi}\right)+\mathcal{O}(d-4),$$

$$\theta(-\mathcal{P}^2)\mathcal{J}^{\pi\pi}(\mathcal{P}^2;M^2)=-2L-\frac{1}{16\pi^2}\left(-1+\ln\frac{M^2}{\mu^2}-\frac{(\Delta-\mathcal{P}^2)}{2\mathcal{P}^2}\ln\frac{M^2}{M_\pi^2}+\frac{\Lambda^{1/2}(\mathcal{P}^2;M^2,M_\pi^2)}{-2\mathcal{P}^2}\ln\left[\frac{(\Lambda^{1/2}-\mathcal{P}^2)^2-\Delta^2}{(\Lambda^{1/2}+\mathcal{P}^2)^2-\Delta^2}\right]\right),$$

$$(\Delta\equiv M^2-M_\pi^2;\ \Lambda(\mathcal{P}^2;M^2,M_\pi^2)\equiv[\mathcal{P}^2-(M-M_\pi)^2][\mathcal{P}^2-(M+M_\pi)^2]), \quad (B8)$$

$$I_1\equiv\mathcal{J}^{\pi\pi}(-M_\pi^2,M_\pi^2)=-2L-\frac{1}{16\pi^2}\left[-1+\ln\frac{M_\pi^2}{\mu^2}+\sqrt{5}\ln\left(\frac{\sqrt{5}+1}{\sqrt{5}-1}\right)\right], \quad (B9)$$

$$I_8\equiv\mathcal{J}^{\pi\pi}(\mathcal{P}^2=0;M^2=M_\pi^2)=-2L-\frac{1}{16\pi^2}\left(1+\ln\frac{M_\pi^2}{\mu^2}\right)+\mathcal{O}(d-4), \quad (B10)$$

$$\theta(-P^2)\frac{\partial}{\partial M^2}\mathcal{J}^{\pi\pi}(P^2;M^2,M_\pi^2)|_{M^2=M_\pi^2}=-\frac{1}{16\pi^2}\left(\frac{1}{M_\pi^2}+\frac{1}{\sqrt{(-P^2)(4M_\pi^2-P^2)}}\ln\left[\frac{\sqrt{4M_\pi^2-P^2}+\sqrt{-P^2}}{\sqrt{4M_\pi^2-P^2}-\sqrt{-P^2}}\right]\right),\quad\text{(B11)}$$

$$\text{(i)}\quad\gamma_0(\omega=0,\Omega=M_\pi,P^2=0)-\gamma_0(\omega=0,\Omega=-M_\pi,P^2=0)=-\frac{1}{32M_\pi},\quad\text{(B12)}$$

$$\text{(ii)}\,I_{11}\equiv\gamma_0(\omega=-M_\pi,\Omega=0,P^2=-M_\pi^2)=\frac{1}{8\sqrt{2}\,\pi M_\pi}\left[\ln\left(1+\frac{3+\sqrt{5}}{2}\right)\frac{(\sqrt{5}+1)}{\sqrt{3+\sqrt{5}}}-\ln\left(1+\sqrt{\frac{3-\sqrt{5}}{2}}\right)\frac{(\sqrt{5}-1)}{\sqrt{3-\sqrt{5}}}\right]$$

$$=\frac{1}{8\pi M_\pi}\ln\left[\frac{1+\sqrt{5}}{2}\right].\quad\text{(B13)}$$

I_{11} is a *new* integral that one needs to evaluate for the DCX one-loop graphs. For values of $P^2\neq 0,-M_\pi^2$, one gets the following expressions, which are also *new*:

$$\text{(i)}\quad\gamma_0(\omega=-M_\pi,\Omega=-M_\pi,P^2=M_\pi^2-\vec{P}^2)-\gamma_0(\omega=M_\pi,\Omega=M_\pi,P^2=M_\pi^2-\vec{P}^2)$$

$$=-\frac{1}{2\pi|\vec{P}|}\left[\arctan\left[\frac{M_\pi}{\sqrt{M_\pi^2+\vec{P}^2}}\right]-\frac{|\vec{P}|}{\sqrt{M_\pi^2+\vec{P}^2}}\sum_{k=0}^\infty\frac{(2k)!}{2^{2k}(k!)^2(2k+1)}F_1\left(\frac{3}{2},k+1,1,2;-\frac{\vec{P}^2}{M_\pi^2},\frac{M_\pi^2}{[2M_\pi^2+\vec{P}^2]}\right)\right],$$

$$\text{(B14)}$$

where

$$F_i(a,b,c,d;x,y)\equiv\text{Appell functions}\;(i=1,2,3,4),$$

$$F_1(a,b,c,d;x,y)=\sum_{m=0}^\infty\sum_{n=0}^\infty\frac{a_{m+n}b_m c_n}{c_{m+n}}\frac{x^m y^n}{m!n!},\quad\text{(B15)}$$

$$\text{(ii)}\quad\gamma_0(\omega=-M_\pi,\Omega=0,P^2=-\vec{P}^2)=\frac{\left[1+\frac{\vec{P}^2}{2M_\pi^2}-\frac{|\vec{P}|}{M_\pi}\sqrt{4+\frac{\vec{P}^2}{M_\pi^2}}\right]}{16\pi^2|\vec{P}|\sqrt{4+\frac{\vec{P}^2}{M_\pi^2}}}\sum_{k=0}^\infty\frac{(2k)!}{(k!)^2 2^{2k}(2k+1)}\left[2B\left(k+2,\frac{1}{2}\right)\,_2F_1\left(k+2,1;k\right.\right.$$

$$\left.+\frac{5}{2};\frac{\left[-\frac{\vec{P}^2}{2M_\pi^2}+\sqrt{4+\frac{\vec{P}^2}{M_\pi^2}}\right]}{\left[-\left(1+\frac{\vec{P}^2}{2M_\pi^2}\right)+\sqrt{4+\frac{(\vec{P}^2)}{M_\pi^2}}\right]}\right)$$

$$\left.-B\left(k+1,\frac{1}{2}\right)\,_2F_1\left(k+1,1;k+\frac{3}{2};\frac{\left[-\frac{\vec{P}^2}{2M_\pi^2}+\sqrt{4+\frac{\vec{P}^2}{M_\pi^2}}\right]}{\left[-\left(1+\frac{\vec{P}^2}{2M_\pi^2}\right)+\sqrt{4+\frac{\vec{P}^2}{M_\pi^2}}\right]}\right)\right]$$

$$-\frac{1}{16\pi^2|\vec{P}|\sqrt{4+\dfrac{\vec{P}^2}{M_\pi^2}}}\sum_{k=0}^{\infty}\frac{(2k)!}{(k!)^2 2^{2k}(2k+1)}\int_0^1 dx\,\frac{x^k(2x-1)}{\sqrt{1-x}}$$

$$\times\frac{1}{\left(x-\dfrac{\left[\left(1+\dfrac{\vec{P}^2}{2M_\pi^2}\right)+\sqrt{4+\dfrac{\vec{P}^2}{M_\pi^2}}\,\dfrac{|\vec{P}|}{M_\pi}\right]}{\left[\dfrac{\vec{P}^2}{2M_\pi^2}+\sqrt{4+\dfrac{\vec{P}^2}{M_\pi^2}}\,\dfrac{|\vec{P}|}{M_\pi}\right]}\right)}. \tag{B16}$$

2. Other integrals

The results obtained after evaluation of other integrals of Eqs. (B2) and (B3) are given below.

(a) 2π-*propagator integrals.* The following relations, (B20), (B22), (B24), (B26), and (B28), are not explicitly given in the literature. These relations are absolutely general and become relevant when evaluating the off-threshold one-loop amplitudes for kinematic points away from Eqs. (17):

$$I_9\equiv\mathcal{J}_2^{\pi\pi}(0,M_\pi^2)=-\frac{1}{2}\Delta_\pi(M^2,0), \tag{B17}$$

$$I_{10}\equiv\mathcal{J}_3^{\pi\pi}(0,M_\pi^2)=\frac{1}{3}\mathcal{J}^{\pi\pi}(0,M_\pi^2)\equiv\frac{1}{3}I_8, \tag{B18}$$

$$\mathcal{J}_1^{\pi\pi}(\mathcal{P}^2,M^2)=\frac{1}{2\mathcal{P}^2}[\Delta_\pi(0,M^2)-\Delta_\pi(0,M_\pi^2)+(\Delta+\mathcal{P}^2)\mathcal{J}(\mathcal{P}^2,M^2)],$$

$$I_2\equiv\mathcal{J}_1^{\pi\pi}(-M_\pi^2,M_\pi^2)=\frac{1}{2}\mathcal{J}^{\pi\pi}(-M_\pi^2,M_\pi^2)=-L-\frac{1}{32\pi^2}\left[-1+\ln\frac{M_\pi^2}{\mu^2}+\sqrt{5}\,\ln\left(\frac{\sqrt{5}+1}{\sqrt{5}-1}\right)\right] \tag{B19}$$

$$-M_\pi^2 I_5\equiv-M_\pi^2\frac{\partial}{\partial M^2}\mathcal{J}_1^{\pi\pi}\Big|_{M^2=M_\pi^2;\mathcal{P}^2=-M_\pi^2}=\frac{1}{2}\left(\frac{\partial}{\partial M^2}\Delta_\pi(0,M^2)-M_\pi^2\frac{\partial}{\partial M^2}\mathcal{J}^{\pi\pi}\right)_{M^2=M_\pi^2;\mathcal{P}^2=-M_\pi^2}+\frac{1}{2}\mathcal{J}^{\pi\pi}(-M_\pi^2,M_\pi^2) \tag{B20}$$

$$=-\frac{L}{2}+\frac{3}{32\pi^2}-\frac{\sqrt{5}}{40\pi^2}\ln\left(\frac{\sqrt{5}+1}{\sqrt{5}-1}\right), \tag{B21}$$

$$\mathcal{J}_2^{\pi\pi}(\mathcal{P}^2;M^2=M_\pi^2)=\frac{\left[\left(2M_\pi^2-\dfrac{\mathcal{P}^2}{2}\right)J^{\pi\pi}(\mathcal{P}^2)-\Delta_\pi(0,M_\pi^2)\right]}{2(d-1)}, \tag{B22}$$

which for $\mathcal{P}^2=-M_\pi^2$ gives

$$I_3\equiv\mathcal{J}_2^{\pi\pi}(-M_\pi^2,M_\pi^2)=-\frac{7M_\pi^2}{6}L+\frac{29}{576\pi^2}M_\pi^2-\frac{7}{192\pi^2}M_\pi^2\ln\frac{M_\pi^2}{\mu^2}-\frac{5\sqrt{5}}{192\pi^2}\ln\left(\frac{\sqrt{5}+1}{\sqrt{5}-1}\right)+\mathcal{O}(d-4), \tag{B23}$$

$$\mathcal{J}_3^{\pi\pi}(\mathcal{P}^2;M^2=M_\pi^2)\equiv J_3^{\pi\pi}(\mathcal{P}^2)=\frac{[(d\mathcal{P}^2-4M_\pi^2)J^{\pi\pi}(\mathcal{P}^2)+2(2-d)\Delta_\pi(0,M_\pi^2)]}{4(d-1)\mathcal{P}^2}, \tag{B24}$$

which for $\mathcal{P}^2=-M_\pi^2$ gives

$$I_4 \equiv \mathcal{J}_3^{\pi\pi}(-M_\pi^2, M_\pi^2) = -\frac{2}{3}L + \frac{19}{288\pi^2} - \frac{1}{48\pi^2}\ln\frac{M_\pi^2}{\mu^2} - \frac{\sqrt{5}}{24\pi^2}\ln\left(\frac{\sqrt{5}+1}{\sqrt{5}-1}\right) + \mathcal{O}(d-4),$$ (B25)

$$\theta(-\mathcal{P}^2)\mathcal{P}^2\frac{\partial}{\partial M^2}\mathcal{J}_2^{\pi\pi}(\mathcal{P}^2; M^2) = \theta(-\mathcal{P}^2)\frac{1}{2(1-d)}\left[-\mathcal{J}^{\pi\pi} - \frac{1}{2}(4M_\pi^2 - \mathcal{P}^2)\frac{\partial}{\partial M^2}\mathcal{J}^{\pi\pi} + \frac{1}{2}\frac{\partial}{\partial M^2}\Delta_\pi(0, M^2)\right]$$

$$= -\frac{L}{2} - \frac{1}{192\pi^2}\left(1 - \frac{\mathcal{P}^2}{M_\pi^2}\right) - \frac{1}{64\pi^2}\ln\frac{M_\pi^2}{\mu^2}$$

$$- \frac{1}{64\pi^2}\sqrt{\frac{[4M_\pi^2 - \mathcal{P}^2]}{-\mathcal{P}^2}}\ln\left[\frac{\sqrt{4M_\pi^2 - \mathcal{P}^2} + \sqrt{-\mathcal{P}^2}}{\sqrt{4M_\pi^2 - \mathcal{P}^2} - \sqrt{-\mathcal{P}^2}}\right] + \mathcal{O}(d-4).$$ (B26)

So,

$$I_6 \equiv \frac{\partial}{\partial M^2}\mathcal{J}_2^{\pi\pi}(-M_\pi^2, M_\pi^2)|_{M^2 = M_\pi^2} = -\frac{L}{2} - \frac{1}{96\pi^2} - \frac{1}{64\pi^2}\ln\frac{M_\pi^2}{\mu^2} - \frac{\sqrt{5}}{64\pi^2}\ln\left(\frac{\sqrt{5}+1}{\sqrt{5}-1}\right),$$ (B27)

$$M_\pi^2\frac{\partial}{\partial M^2}\mathcal{J}_3^{\pi\pi}\bigg|_{M^2 = M_\pi^2} = \left(d\frac{\partial}{\partial M^2}\mathcal{J}_2^{\pi\pi} - M^2\frac{\partial}{\partial M^2}\mathcal{J}^{\pi\pi}\right)\bigg|_{M^2 = M_\pi^2} - \mathcal{J}^{\pi\pi}.$$ (B28)

So,

$$I_7 \equiv \frac{\partial}{\partial M^2}\mathcal{J}_3^{\pi\pi}(-M_\pi^2, M_\pi^2)|_{M^2 = M_\pi^2} = -\frac{7}{96\pi^2} + \frac{1}{16\sqrt{5}}\ln\left(\frac{\sqrt{5}+1}{\sqrt{5}-1}\right).$$ (B29)

(b) 2π–*one-nucleon–propagator integrals.* The following relations, (B30), (B32), and (B35), are not explicitly given in the literature, and are absolutely general and become relevant when evaluating the off-threshold one-loop amplitudes for kinematic points away from Eq. (17).

$$\gamma_1(\omega, \Omega, \mathcal{P}^2) = \frac{[2\mathcal{P}^2 J^{\pi\pi}(\mathcal{P}^2) + \mathcal{P}^2(2\omega - \Omega)\gamma_0(\omega, \Omega, \mathcal{P}^2) - \Omega(J^{\pi N}(\omega) - J^{\pi N}(\omega - \Omega))]}{2(\mathcal{P}^2 - \Omega^2)},$$

$$\gamma_2(\omega, \Omega, \mathcal{P}^2) = \frac{[J^{\pi N}(\omega) - J^{\pi N}(\omega - \Omega) - 2\Omega J^{\pi\pi}(\mathcal{P}^2) + (\mathcal{P}^2 - 2\omega\Omega)\gamma_0(\omega, \Omega, \mathcal{P}^2)]}{2(\mathcal{P}^2 - \Omega^2)}.$$ (B30)

Hence,

$$I_{12} \equiv \gamma_2(0, -M_\pi, 0) - \gamma_2(0, M_\pi, 0) = \frac{1}{4M_\pi\pi^2},$$ (B31)

$$\gamma_3(\omega, \Omega, \mathcal{P}^2) = \frac{[2M_\pi^2\gamma_0(\omega, \Omega, \mathcal{P}^2) - 2\omega\gamma_1(\omega, \Omega, \mathcal{P}^2) - \mathcal{P}^2\gamma_2(\omega, \Omega, \mathcal{P}^2) - J^{\pi N}(\omega - \Omega)]}{2(d-2)}$$

$$= \frac{1}{4}[2M_\pi^2\gamma_0(\omega, \Omega, \mathcal{P}^2) - 2\omega\gamma_1(\omega, \Omega, \mathcal{P}^2) - \mathcal{P}^2\gamma_2(\omega, \Omega, \mathcal{P}^2) - J^{\pi N}(\omega - \Omega)] - \frac{(2\omega - \Omega)}{32\pi^2} + \mathcal{O}(d-4).$$ (B32)

Hence,

$$\gamma_3(\omega=0,\Omega=-M_\pi,\mathcal{P}^2=M_\pi^2-\vec{P}^2)-\gamma_3(\omega=0,\Omega=M_\pi,\mathcal{P}^2=M_\pi^2-\vec{P}^2)$$

$$=\frac{1}{4}\left[\left(\gamma_0(0,-M_\pi,M_\pi^2-\vec{P}^2)\right.\right.$$

$$\left.-\gamma_0(0,M_\pi,M_\pi^2-\vec{P}^2)\right)\frac{[M_\pi^2+\vec{P}^2]^2}{2\vec{P}^2}+\frac{[M_\pi^2+\vec{P}^2]}{2\vec{P}^2}(J^{\pi N}(-M_\pi)-J^{\pi N}(M_\pi))\right]$$

$$-\frac{M_\pi}{16\pi^2}+\mathcal{O}(d-4). \tag{B33}$$

Thus,

$$I_{13}\equiv\gamma_3(0,-M_\pi,0)-\gamma_3(0,M_\pi,0)=2LM_\pi+M_\pi\left(\frac{1}{64}-\frac{1}{8\pi^2}\right)+\frac{M_\pi}{16\pi^2}\ln\frac{M_\pi^2}{\mu^2}+\mathcal{O}(d-4). \tag{B34}$$

Now,

$$\gamma_5(\omega,\Omega,\mathcal{P}^2)=-\frac{1}{2(d-2)(\mathcal{P}^2-\Omega^2)}[(d-2)\Omega J^{\pi\pi}(\mathcal{P}^2)+2\gamma_2(\omega,\Omega,\mathcal{P}^2)[(d-1)\mathcal{P}^2+\omega\Omega(d-2)]+(d-3)J^{\pi N}(\omega-\Omega)$$

$$-2\omega\gamma_1(\omega,\Omega,\mathcal{P}^2)+2M_\pi^2\gamma_0(\omega,\Omega,\mathcal{P}^2)]$$

$$=\frac{1}{4(\mathcal{P}^2-\Omega^2)}\left[2\omega\gamma_1(\omega,\Omega,\mathcal{P}^2)-2\Omega J^{\pi\pi}+(3\mathcal{P}^2-4\omega\Omega)\gamma_2(\omega,\Omega,\mathcal{P}^2)-J^{\pi N}(\omega-\Omega)\right.$$

$$\left.-2M_\pi^2\gamma_0(\omega,\Omega,\mathcal{P}^2)+\frac{(2\omega-\Omega)}{8\pi^2}\right]+\mathcal{O}(d-4). \tag{B35}$$

Hence,

$$\gamma_5(\omega=0,\Omega=-M_\pi,\mathcal{P}^2=M_\pi^2-\vec{P}^2)-\gamma_5(\omega=0,\Omega=M_\pi,\mathcal{P}^2=M_\pi^2-\vec{P}^2)$$

$$=-\frac{1}{4\vec{P}^2}\left[-\frac{[3M_\pi^2-5\vec{P}^2]}{2\vec{P}^2}(J^{\pi N}(-M_\pi)-J^{\pi N}(M_\pi))-\frac{(3[M_\pi^2-\vec{P}^2]^2+4M_\pi^2\vec{P}^2)}{2\vec{P}^2}(\gamma_0(0,-M_\pi,M_\pi^2-\vec{P}^2)\right.$$

$$\left.-\gamma_0(0,M_\pi,M_\pi^2-\vec{P}^2))+\frac{2M_\pi[5M_\pi^2-3\vec{P}^2]}{\vec{P}^2}\mathcal{J}^{\pi\pi}(M_\pi^2-\vec{P}^2)+\frac{M_\pi}{4\pi^2}\right]+\mathcal{O}(d-4). \tag{B36}$$

Thus,

$$I_{14}\equiv\gamma_5(0,-M_\pi,0)-\gamma_5(0,M_\pi,0)=\frac{1}{16\pi^2 M_\pi}+\frac{1}{64M_\pi}+\mathcal{O}(d-4). \tag{B37}$$

---

[1] S. R. Beane, C. Y. Lee, and U. van Kolck, Phys. Rev. C **52**, 2914 (1995).

[2] B.-Y. Park, F. Myhrer, J. R. Morones, T. Meissner, and K. Kubodera, Phys. Rev. C **53**, 1519 (1996).

[3] J. Gasser and H. Leutwyler, Ann. Phys. (N.Y.) **158**, 142 (1984).

[4] V. Bernard, N. Kaiser, and Ulf-G. Meissner, Phys. Lett. B **309**, 421 (1993).

[5] M. F. Jiang and D. S. Koltun, Phys. Rev. C **42**, 2662 (1990).

[6] V. Bernard, N. Kaiser, and Ulf-G. Meissner, Int. J. Mod. Phys. E **4**, 193 (1995).

[7] S. Weinberg, Phys. Lett. B **251**, 288 (1990).

[8] S. Weinberg, Phys. Lett. B **295**, 114 (1992).

[9] David B. Kaplan, Martin J. Savage, and Mark B. Wise, Phys. Lett. B **424**, 390 (1998).

[10] David B. Kaplan, Martin J. Savage, and Mark B. Wise, Nucl. Phys. **B534**, 329 (1998).

[11] V. Bernard, N. Kaiser, and Ulf-G. Meissner, Nucl. Phys. **B457**, 147 (1995).

[12] M. G. Olsson and L. Turner, Phys. Rev. Lett. **20**, 1127 (1968).

[13] J. Gasser, M. E. Sainio, and A. Svarc, Nucl. Phys. **B307**, 779 (1988).